Inorganic Chemistry

Article

pubs.acs.org/IC

Bispidine Analogues of Cisplatin, Carboplatin, and Oxaliplatin. Synthesis, Structures, and Cytotoxicity

Huiling Cui,[†] Richard Goddard,[†] Klaus-Richard Pörschke,*[,†] Alexandra Hamacher,[‡] and Matthias U. Kassack[‡]

[†]Max-Planck-Institut für Kohlenforschung, Kaiser-Wilhelm-Platz 1, D-45470 Mülheim an der Ruhr, Germany

[‡]Institut für Pharmazeutische und Medizinische Chemie der Heinrich-Heine-Universität Düsseldorf, Universitätsstrasse 1, 40225 Düsseldorf, Germany

Supporting Information

ABSTRACT: Bispidine (3,7-diazabicyclo[3.3.1]nonane, $C_7H_{14}N_2$) analogues of cisplatin, carboplatin, and oxaliplatin have been prepared. $(C_7H_{14}N_2)PtCl_2$·DMF (**1b**), obtained from (1,5-hexadiene)$PtCl_2$ and bispidine in DMF, is dimeric in the solid state. Dissolving **1b** in hot *N*-methylformamide allows crystallization of the solvent-free polymeric $(C_7H_{14}N_2)PtCl_2$ (**1a**). Recrystallization of **1a,b** from hot water yields the trihydrate $(C_7H_{14}N_2)PtCl_2·3H_2O$ (**1c**). Reaction of **1** with Ag_2(cbdca) (cbdca = 1,1-cyclobutanedicarboxylate) in water affords the pentahydrate $(C_7H_{14}N_2)Pt\{C_4H_6(CO_2)_2\}·5H_2O$ (**2b**), which loses water in vacuo to give $(C_7H_{14}N_2)Pt\{C_4H_6(CO_2)_2\}$ (**2a**). Reaction of **1** with $AgNO_3$ in water, followed by addition of $Na_2C_2O_4$, affords the water-free polymeric $(C_7H_{14}N_2)Pt(C_2O_4)$ (**3**). All complexes have been structurally characterized, revealing various patterns of N−H···Cl and N−H···O hydrogen bonds. In the hydrates **1c** and **2b** the complexes are embedded in intricate three-dimensional water networks. Complexes **1a**, **2a**, and **3** have been tested for their cytotoxicity against human cancer cell lines K562 (chronic myeloid leukemia), A2780 (ovarian cancer), and its platinum-resistant subline A2780 CisR and are compared to their parent analogues. The new complexes show significant cytotoxic activity along with a low platinum resistance factor.

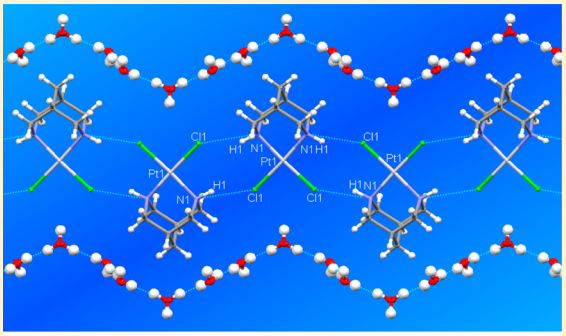

INTRODUCTION

The serendipitous discovery of the antitumor activity of cisplatin, *cis*-$(NH_3)_2PtCl_2$,[1] by Rosenberg and his co-workers[2] prompted an intense screening of related Pt complexes in a search for possibly more effective and less toxic analogues. In chemotherapy, the prototypical cisplatin[3,4] (Figure 1) is

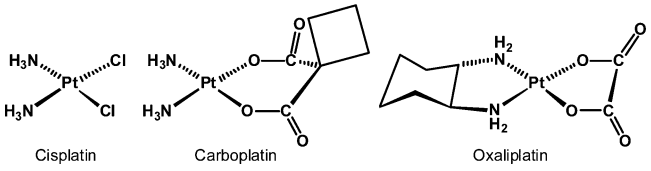

Figure 1. Worldwide-approved platinum drugs for cancer therapy.

curative in the treatment of testicular cancer and also particularly active in the treatment of ovarian, cervix, and bladder cancers and palliative in the treatment of metastatic head, neck, breast, and various forms of lung cancer. Substantial side effects are dose-limiting nephrotoxicity, gastrointestinal toxicity, ototoxicity, neurotoxicity, and myelosuppression.[5] Patients experience inter alia nausea, vomiting, and anorexia, which are only partially alleviated by antiemetics. Other adverse effects include numbness, tinnitus, and reduced hearing. Major enduring problems are inherent platinum resistance (e.g., in the case of colon cancer) and the development of acquired platinum resistance of refractory tumors (see also below).[6] Various X-ray structure determinations have been performed on cisplatin[7a,b] and some base adducts.[7c−f] However, no crystalline *hydrates* of cisplatin have been observed so far.

From early screenings carboplatin[8a] emerged as an alternative platinum-based and clinically applied second-generation anticancer agent.[9] In carboplatin the rather labile chloride anions of cisplatin are replaced by 1,1-cyclobutanedicarboxylate (cbdca), a dianionic substituted malonate ligand. Carboplatin exhibits a lower reactivity and slower DNA binding kinetics than cisplatin and as a consequence has fewer side effects. Otherwise, carboplatin has a very similar activity profile against cancers but is generally less active.[5] It appears to act with cellular DNA in a way quite similar to that of cisplatin. The major drawbacks are that carboplatin does not solve the problem of platinum resistance and its myelosuppressive effect. The latter causes the blood cell and platelet output of bone marrow to decrease quite dramatically, sometimes to as low as

Received: October 31, 2013
Published: March 25, 2014

   dx.doi.org/10.1021/ic402737f | *Inorg. Chem.* 2014, 53, 3371−3384

10% of its usual production levels. Clinically, the lower activity of carboplatin is usually overcome by delivering a 4-fold dosage as compared to cisplatin. Due to its relative inertness, most of the carboplatin remains unaltered in the bloodstream and becomes egested in urine. The crystal structures of carboplatin[8b,c] and numerous other Pt−cbdca complexes[10,11c] are known. In addition, various other Pt−malonate complexes,[12] including $(NH_3)_2Pt(malonate)$,[13] have been structurally investigated.

Oxaliplatin,[14] (*trans*-(*R*,*R*)-1,2-diaminocyclohexane)-platinum(II) oxalate, is considered to be a third-generation Pt-based anticancer drug. Instead of NH_3, oxaliplatin contains the chiral *trans*-1,2-diaminocyclohexane (DACH) ligand as the neutral "carrier ligand". Whereas the also potent Pt−dichloride $(DACH)PtCl_2$ scarcely dissolves in water, the oxalate $(DACH)Pt(C_2O_4)$ is more soluble. Since 1998 oxaliplatin has gained almost worldwide approval for the treatment of colon cancers. The dose-limiting toxicity is neurotoxicity.[5c,d] Interestingly, the *trans*-(*R*,*R*) enantiomer is more potent than the *trans*-(*S*,*S*) enantiomer and both of these are more efficient than the *cis*-(*R*,*S*) isomer.[15] The efficacy of the trans isomers is attributed both to the relatively flat structures, allowing for an easier approach of the trans isomeric complexes to cellular DNA, and to the specific hydrogen bonding between the primary amine N−H functions and DNA purine bases. Nevertheless, the steric constraint imposed by this chelate ligand appears to impede recognition and repair of DNA damage by specific cell proteins, resulting in reduced platinum resistance in comparison to the first- and second-generation drugs. Numerous substituted oxaliplatin derivatives have been investigated.[16] In addition to the structure of oxaliplatin,[17] the structures of $(DACH)PtCl_2 \cdot DMF$[18] and other $(DACH)PtX_2$ complexes,[10a,19] as well as of $(NH_3)_2Pt(oxalate)$[13] and other Pt−oxalate complexes,[20] have been determined.

The mechanism of action of these drugs inside the body is known in much detail.[21] The neutral drug, which must show sufficient water solubility, is stable in the bloodstream. Accumulation in the cell has been traditionally attributed to passive diffusion, but recent evidence suggests that a series of transport mechanisms are also at play.[22] For migration through the cell membrane high lipophilicity seems important, which may be imparted by the amine as a "carrier ligand", if possible supported by the anion. Inside the cell hydrolysis of the anionic ligand(s) occurs and an aqua complex, e.g., $[cis\text{-}(NH_3)_2Pt(H_2O)Cl]^+$, is formed which targets the DNA. Eventually, the $[cis\text{-}(amine)_2Pt^{2+}]$ entity becomes coordinated to two N7 atoms of contiguous guanine bases of a single DNA strand, leading to a kink and partial unwinding of the DNA.[23] Platinum resistance seems due to an array of mechanisms, including reduced accumulation and enzymatic DNA repair by the cell.[24] Cross-resistance of cisplatin and carboplatin is attributed to formation of the common $[cis\text{-}(NH_3)_2Pt]^{2+}$ entity, whereas the DACH ligand of oxaliplatin impedes cross-resistance.

There is a vivid ongoing search for new platinum drugs (as well as for drugs of other metals, e.g., ruthenium) aimed at mitigating the side effects, overcoming inherent or acquired platinum resistance of the tumor, broadening the spectrum of antitumor activity, improving the targeting, and simplifying administration of the drug. In these studies the platinum complexes are modified with respect to the neutral amine carrier ligand, the anionic leaving group, oxidation state, geometric features, multimetal structures, and so forth.[4,25] Structure−activity relationships in the "classical" type of platinum cytostatics were first established by Cleare and Hoeschele from empirical studies.[26] Activity is found for complexes which are neutral and obey the general formula *cis*-$Pt^{II}A_2X_2$, in which A represents a neutral amine ligand bearing one to three protons and X (X_2, respectively) represents an anionic leaving group such as halide, oxalate, and malonate which only slowly hydrolyzes. The amine as the carrier ligand always remains coordinated.

The reason for the necessity of the presence of NH functions for the Pt drug is seen in various forms of N−H···O hydrogen bonds, which may trigger (a) the preselection of DNA as the target molecule as opposed to the various proteins contained in the cell, e.g., by N−H···O hydrogen bonding to the DNA backbone phosphate, (b) the selection of the guanosine versus the adenosine binding site within the DNA by anchoring the drug at the guanine O6 atom by N−H···O6 hydrogen bonding, and (c) strengthening of the adduct formed by Pt(II) (after hydrolysis of the anionic ligand) with the guanine N7 atom by the chelate effect involving the N−H···O6 bond (Figure 2).[27]

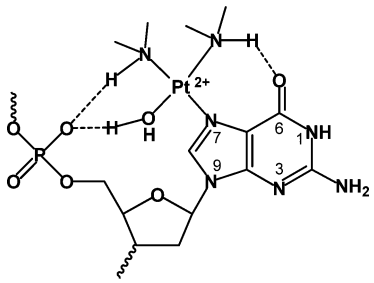

Figure 2. Schematic drawing of possible interactions of a $[(R_2NH)_2Pt(H_2O)]^{2+}$ moiety with N7 and O6 of a guanine ligand and phosphate of the DNA backbone.

Reduced steric strain, in comparison to the situation for a tertiary amine, must also be taken into account, with respect to both the process of approaching the DNA and the structure of the final intrastrand complex. In addition, the aqua ligand at Pt(II) is also expected to be involved in hydrogen bonding. An impressive example for the formation of a N−H···O6 hydrogen bond as part of a chelate complex was shown by the X-ray structure determination of a chiral $(DACH)Pt^{II}$ 1,2-intrastrand cross-link in a DNA duplex, in which the pseudoequatorial NH of the DACH ligand forms such a bond.[18]

Ammine as a diligand provides three protons at each N atom, allowing for the highest flexibility in N−H···O hydrogen bonding. Such flexibility is reduced for bidentate primary amines, and the rather rigid DACH ligand uses only one of the four NH functions to form the specific N−H···O6 bond. A series of Pt(II) complexes having secondary amine ligands such as cyclic monoamines[11] and chelating acyclic[28] and cyclic diamines[29] have also been investigated with respect to their structure and cytostatic properties, although such complexes are generally expected to be less potent. Typical examples for a cyclic diamine ligand are 1,4-diazacycloheptane[29b,f] (**B**) and its C-substituted derivatives.[29c,d] Pt(II) complexes having the parent piperazine (**A**)[30] or 1,5-diazacyclooctane (**C**) as a chelating ligand have apparently not been reported so far. The latter would be expected to assume a chair−boat conformation of the chelate substructures to avoid 3,8-transannular strain. In particular, complexes of types **B** and **C** can be expected to impose unduly high steric constraint when penetrating the cell membrane, for example.

dx.doi.org/10.1021/ic402737f | Inorg. Chem. 2014, 53, 3371−3384

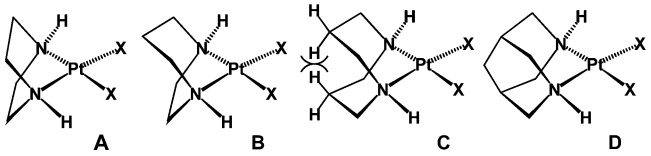

Replacement of the two transannular interfering hydrogen atoms in **C** by carbon compresses the ligand and leads to bispidine-type (3,7-diazabicyclo[3.3.1]nonane type) ligands as in **D**, which are more compact than the ligands in either **B** or **C**. The structure of the bispidine in **D** appears among the smallest conceivable for a chelating bicyclic secondary diamine.

As possible advantages of the bispidine structure, one may envisage the following.

(i) The adamantane-type structural element of the bispidine with the Pt atom comprises a completely rigid and utmost strong ligand to metal coordination.

(ii) The substituents at nitrogen are tied back by the bicyclic structure, exposing the secondary amine protons. The protons lie perforce at fixed positions in the coordination plane of the metal.

(iii) The strong binding and high basicity of the bispidine ligand might influence the kinetics of the Pt−X bond cleavage in the cell.

(iv) Tumor tissue is more permeable toward macromolecules than normal tissue and tends to retain these (enhanced permeability and retention effect, EPR).[2Sa,b] For a cisplatin-type drug with a relatively bulky diamine carrier such as bispidine, the possible occurrence of an EPR effect could lead to a specific accumulation of the drug in tumor tissue.

(v) In comparison to cisplatin, bispidine as a "more organic" carrier should confer an increased lipophilicity to a derivative drug, similar to the case for carboplatin (for its leaving ligand) and oxaliplatin (for its DACH carrier ligand). High lipophilicity will improve penetration of the platinum drug into the tumor cell (endocytosis).[2Sa,b]

(vi) High hydrolysis stability and high lipophilicity, expected for a bispidine-derived drug, would be required for oral administration and intestinal uptake.[31]

(vii) While cisplatin and carboplatin both give rise to $[(NH_3)_2Pt]^{2+}$ as the DNA-binding species, the corresponding species for oxaliplatin and a bispidine-derived drug should be different. Consequently, reduced cross-resistance with both cisplatin and carboplatin on one side and oxaliplatin on the other can be expected.

In nature, the bispidine skeleton is found in numerous alkaloids, of which (−)-sparteine and cytisine are the most noteworthy.[32] These are physiologically highly active and toxic when swallowed, but some of them have also been tested for various therapeutic properties. There are countless reports of natural or synthetic bispidines coordinated to transition metals.[33] However, although a few thousand platinum complexes have been tested for their antitumor activity, surprisingly complexes with bispidine-derived carriers appear not to be among them. The possible antitumor activity of 1,5-diphenyl-substituted Pt−bispidin-9-one complexes was considered as early as 1995, but no details were given.[34] For the parent bispidine, the first transition metals were prepared by Stetter and Merten in 1957,[35] but no systematic study seems to have been performed since then.

Guided by these considerations, we thought it worthwhile to investigate whether the parent bispidine[36,37] might be a suitable ligand for Pt(II) and to determine what chemical, physical, and biological properties the complexes might have. We have therefore synthesized the series of Pt−bispidine analogues **1**−**3** (Figure 3) of cisplatin, carboplatin, and oxaliplatin, some containing DMF and water solute molecules. We will show that the compounds have interesting solid-state structures and incorporate a reduced but significant cytotoxic activity in comparison with cisplatin.

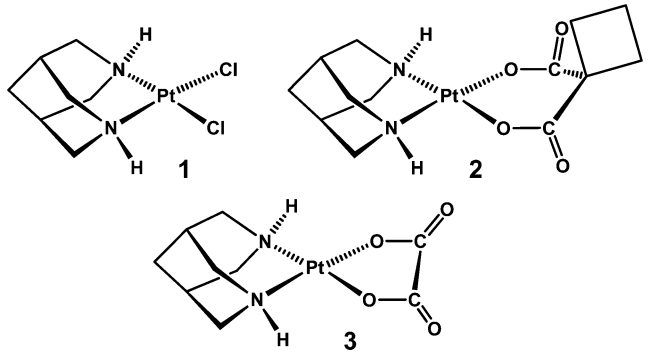

Figure 3. Bispidine-modified analogues **1**−**3** of cisplatin, carboplatin, and oxaliplatin.

RESULTS AND DISCUSSION

Synthesis of the New Pt−Bispidine Complexes 1−3. In a previous study[34] (1,5-hexadiene)$PtCl_2$[38] was reacted with 1,5-diphenyl-substituted bispidin-9-ones $Ph_2C_7H_8O(NR)_2$ (R = H, Me) by prolonged refluxing in $CHCl_3$ to afford the complexes $\{Ph_2C_7H_8O(NR)_2\}PtCl_2$ in moderate yield (40−46%). These complexes were also converted into the iodides.[34]

For the synthesis of the Pt−bispidine analogue of cisplatin, we reacted (1,5-hexadiene)$PtCl_2$ with the parent bispidine ($C_7H_{14}N_2$) in DMF at 70 °C for 3 h. Displacement of the 1,5-hexadiene ligand results in an intensely yellow reaction solution. Slow recooling of the solution to ambient temperature afforded large pale yellow crystals of the DMF adduct $(C_7H_{14}N_2)PtCl_2$·DMF (**1b**) in 87% yield (Scheme 1). No byproducts were detected in the mother liquor (NMR). An X-ray structure determination revealed the cocrystal **1b**, in which a DMF molecule is bound to a bispidine ligand by a N−H···$OCHNMe_2$ hydrogen bond (see below). The interaction appears to be weak, since DMF (bp 153 °C) can be fully removed under vacuum at 50 °C within 24 h to give solvent-free $(C_7H_{14}N_2)PtCl_2$ (**1a**). The latter recrystallizes from the less basic *N*-methylformamide (NMF) without inclusion of solvent. Considering that cisplatin forms a weak adduct with NMF,[7b] the NH hydrogen atoms of the bispidine ligand in **1a** are apparently less protic than those of the ammonia ligands in cisplatin. No direct synthesis of **1a** in NMF following Scheme 1 was possible, owing to substantial decomposition of the reaction mixture under these conditions.

While complexes **1a**,**b** appear insoluble in most solvents at ambient temperature, including CH_2Cl_2 and THF, they dissolve increasingly well in water, DMF, and DMSO, particularly when warmed (50 °C). $(C_7H_{14}N_2)PtCl_2·3H_2O$ (**1c**) crystallizes from warm water at ambient temperature, with only little hydrolysis of the Pt−Cl bonds (NMR). In DMSO compounds **1a**−**c** undergo partial solvolysis in an equilibrium reaction to form the ionic $[(C_7H_{14}N_2)Pt(Me_2SO)Cl]Cl$ (**1′**) (eq 1) without obvious byproducts (as verified in DMSO-d_6 by NMR). Such an

dx.doi.org/10.1021/ic402737f | Inorg. Chem. 2014, 53, 3371−3384

Scheme 1

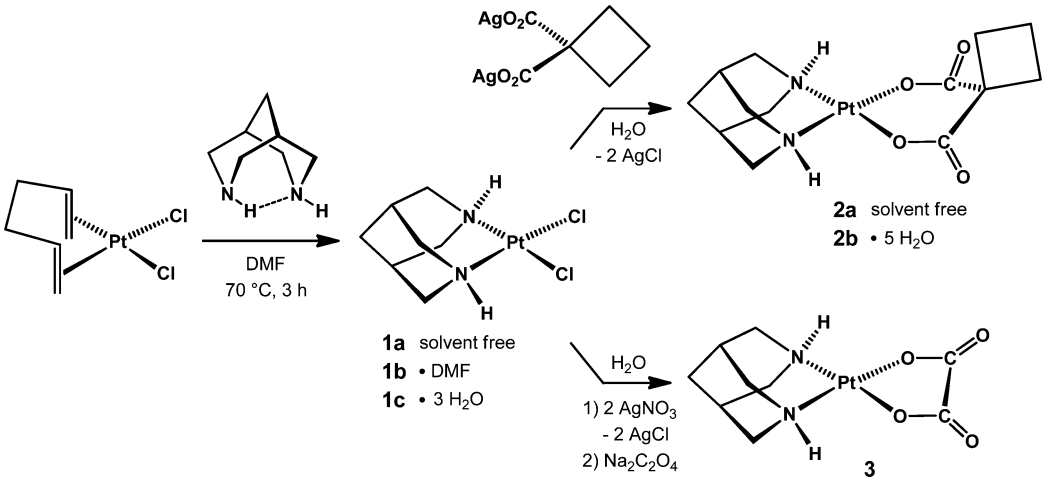

equilibrium has been established previously for cisplatin, although accompanied by various side reactions.[39]

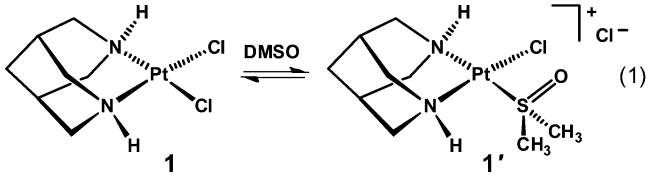

(1)

Synthesis of the Pt–bispidine analogue of carboplatin, $(C_7H_{14}N_2)Pt\{(O_2C)_2C_4H_6\}$ (**2a**), was effected by stirring a suspension of complex **1** and an equimolar amount of $Ag_2(cbdca)$[10e] in water in the dark at ambient temperature for 2 days (Scheme 1). We found no need to first convert **1** into the iodide.[10c] The malonate product complex is more soluble in water than the dichloride **1** and remains in solution when the precipitated AgCl is removed by filtration. Rapid evaporation of the water under vacuum by heating the vessel to 50 °C leaves quantitatively solute-free pure **2a**. Recrystallization of the compound from a smaller amount of water affords the pentahydrate $(C_7H_{14}N_2)Pt\{(O_2C)_2C_4H_6\}\cdot 5H_2O$ (**2b**). Compound **2b** was characterized by an X-ray structure determination, which reveals that the complex is embedded in an intricate network of water molecules (see below).

Similarly, for the synthesis of the Pt–bispidine analogue of oxaliplatin, following a standard protocol,[16] complex **1** was reacted with 2 equiv of $AgNO_3$ in aqueous solution to give, in addition to precipitated AgCl, the soluble diaqua complex $[(C_7H_{14}N_2)Pt(OH_2)_2](NO_3)_2$. Treatment of the latter with disodium oxalate gave poorly soluble $(C_7H_{14}N_2)Pt(C_2O_4)$ (**3**) as a colorless precipitate (Scheme 1). Recrystallization of **3** from hot water afforded thin colorless needles of solute-free **3** in moderate yield (44%).

General Properties of 1–3. The solute-free crystalline solids **1a**, **2a**, and **3** are thermally stable up to 280 °C, as evidenced by DSC. The solute complexes **1b**,**c** and **2b** eliminate the hydrogen-bridge-bonded solute molecules (DMF, H_2O) under vacuum at ambient temperature or above. The best solvents for complexes **1**–**3** are DMSO and H_2O. DMF is also suitable for **1**. Compound **2** dissolves only poorly in DMF, and **3** is almost insoluble in DMF up to 100 °C; therefore, **2** and **3** cannot be satisfactorily recrystallized from this solvent. In solution, the complexes slowly decompose at 100 °C with elimination of platinum black. Decomposition is faster in NMF, in which the complexes also dissolve. The complexes are insoluble in THF, MeCN, and CH_2Cl_2. Unlike the case for **1c** and **2b**, the oxalate **3** does not crystallize from water as a water solute compound.

The complexes are nonvolatile under vacuum; therefore, no EI mass spectra have been recorded. For recording of the ESIpos mass spectrum of the dichloride **1**, DMSO appears to be the best solvent, whereby the mononuclear cation $[(C_7H_{14}N_2)PtCl(DMSO)]^+$ (m/z 434) is found to be the exclusive ion following replacement of one chloride ion by DMSO. In water, cleavage of a Pt–Cl bond is followed by intermolecular Pt–Cl–Pt bridge formation, resulting in $[2\ M - Cl]^+$ (m/z 747) as the base ion. In addition, a series of prominent and associated sodium-containing species such as $[M + Na]^+$ (414, 60%) and $[2\ M + Na]^+$ (805, 40%) were formed, owing to the presence of inadvertently present sodium ions in the instrument. The spectrum of **1** in DMF is uninformative.

Solutions of **2** and **3** in DMSO afford in their ESIpos spectra predominantly the ions $[M + H]^+$, $[M + Na]^+$, $[2\ M + H]^+$, and $[2\ M + Na]^+$ (in addition to some other ions), whereas in water almost exclusively $[M + Na]^+$ and $[2\ M + Na]^+$ are found. The various associated species are indicative of a high strength of the intermolecular bridge bonds. Related ESI MS studies have been previously performed for $(en)PtCl_2$[40c] and Pt(II) amidine[41] complexes.

In the IR spectrum for the uncoordinated bispidine[37] two bands are found at 3400 and 3298 cm^{-1}, attributable to the presence of intermolecular and intramolecular bridging NH···N groups. In contrast, the (solvent-free) complexes **1**–**3** show single bispidine ν(NH) bands at 3180, 3136, and 3161 cm^{-1}, respectively, with the band of the malonate derivative **2** occurring at lowest frequency. While ν(NH) band shifts to lower frequency are typical for secondary amines upon coordination,[42] the extent may also reflect the strength of the various (Pt)N–H···Cl and (Pt)N–H···O bridges in the associated complexes. In addition, for the carboxylate complexes strong and split ν(C=O) bands (**2**, 1623, 1604 cm^{-1}; **3**, 1697, 1659 cm^{-1}) and strong unsplit ν(C–O) bands (**2**, 1360 cm^{-1}; **3**, 1378 cm^{-1}) are observed, in agreement with related complexes.[10c]

NMR Spectra. The ^1H and ^{13}C NMR data of complexes **1**–**3** in various solvents are given in Table 1. The spectra of the

dx.doi.org/10.1021/ic402737f | Inorg. Chem. 2014, 53, 3371–3384

Table 1. ^{1}H and ^{13}C NMR Chemical Shifts (δ) of $(C_7H_{14}N_2)PtCl_2$ (1), $[(C_7H_{14}N_2)PtCl(DMSO)]Cl$ (1′), $(C_7H_{14}N_2)Pt\{C_4H_6(CO_2)_2\}$ (2), and $(C_7H_{14}N_2)Pt(C_2O_4)$ (3) in Various Solvents[a]

compd	solvent	NH	H_e1	H_a1	H2	H3	H6	H7	C1	C2	C3	C4	C5	C6	C7
bispidine[37]	DMSO-d_6	2.44	2.99	2.87	1.38	1.73			52.1	29.0	33.6				
1	DMF-d_7	6.56 (^2J(PtH) 83)	3.48 (^2J(HH) 12.4)	3.15 (^2J(HH) 12.4, ^3J(PtH) 70)	2.20	1.87			54.0	27.4	31.7				
	D_2O	6.57 (^2J(PtH) 77)	3.39 (^2J(HH) 12.3)	2.98 (^2J(HH) 12.3, ^3J(HH) 2.4, ^3J(PtH) 80)	2.19	1.78			53.6	26.5	30.7				
	DMSO-d_6	6.66	3.26 (^2J(HH) 9.1)	2.86 (^2J(HH) 9.1)	2.06	1.69									
1′	DMSO-d_6	7.15, 6.14	3.45, 3.17	3.17, 2.90	2.18	1.78, 1.75									
2	DMSO-d_6	7.24	3.26 (^2J(HH) 12.3)	2.87 (^2J(HH) 12.3)	2.06	1.68	2.65	1.64	53.7	26.2	30.4	177.3	55.4	30.3	14.9
	D_2O		3.33 (^2J(HH) 12.1)	2.92 (^2J(HH) 12.1)	2.13	1.72	2.73	1.75	54.3	26.8	30.6	182.4	56.6	31.5	16.0
3	DMSO-d_6	7.58	3.31 (^2J(HH) 12.3)	2.88 (^2J(HH) 12.3)	2.07	1.70			53.4	26.1	30.4	166.1			
	D_2O		3.36 (^2J(HH) 12.4)	2.93 (^2J(HH) 12.4)	2.15	1.72									

[a]Couplings are given in Hz. Temperature: 25 °C. Assignment:

unadulterated **1** are best recorded in DMF-d_7, since in D_2O partial NH/D exchange with slow hydrolysis of chloride and in DMSO-d_6 partial solvolysis of chloride take place. Complexes **2** and **3** dissolve reasonably well only in DMSO-d_6 for recording of the NMR spectra. All spectra are in agreement with (for **2** time-averaged) C_{2v} symmetry of the complexes in solution. In comparison to the uncoordinated bispidine, the ^{13}C NMR signals of bispidine appear only slightly affected by its coordination to Pt(II).

For complexes **1**−**3** the NH signal is at much lower field (δ(H) 6.5−7.5) than that of the uncoordinated bispidine (δ(H) 2.44). This can be attributed to the more protic nature of NH, resulting from the binding of the free electron pair to Pt(II). For the $C_7H_{12}N_2$ skeleton, in the ^{1}H NMR spectrum separate signals are found for NCH_eH_a, with the axial protons H_a1 resonating at higher field than the equatorial protons H_e1. While both signals are split into doublets due to their geminal coupling ^2J(HH) = 9−12 Hz, H_a1 may show an additional smaller coupling to the bridgehead proton H2. This coupling is attributed to flattening of the chair conformation of the piperidine rings due to the relatively wide N···N opening for Pt(II), which diminishes the dihedral angle between these protons below the ideal 60° and strengthens their vicinal coupling. Couplings of H2 and H3 are not resolved.

A further interesting feature of the ^{1}H NMR spectra of **1** in DMF-d_7 and D_2O are the signals of NH and H_a1, which are flanked by ^{195}Pt coupling satellites,[43] evidencing persistent coordination of the bispidine at Pt. For NH the coupling ^2J(PtH) ≈ 80 Hz can be attributed to the exact location of the hydrogen atom in the coordination plane of Pt(II). For H_a1 the coupling ^3J(PtH) = 70−80 Hz of similar magnitude seems to be due to an almost ideal anti position of H_a1 and ^{195}Pt with respect to the H_a1−C1−N−Pt dihedral angle. The relative intensity of the NH signal in D_2O is less than 1, in comparison with 2 in DMF-d_7, and the signal is markedly broader. There is also a substantial HOD signal, which also indicates slow H/D exchange at NH with the solvent. Interestingly, the ^{13}C NMR signal of the bridgehead C2 appears as a superposition of a triplet and a quintet. This signal seems to be due to ^3J(CD) coupling (3 Hz) of C2 with one and two anti-positioned N−D. For C1 any ^2J(CD) coupling is smaller and is not resolved. Here, however, the signal of C1 has doubled and can be attributed to the isotope effect associated with an about 50% content of ND (signal separation of 0.12 ppm). Assuming that both N atoms of the bispidine remain bound to Pt(II), the H/D exchange can be envisaged by the mechanism suggested in eq 2, consistent with a protic nature of NH. Furthermore,

(2)

additional signals gradually arise in D_2O, which can be attributed to the appearance of a less symmetrical complex, due to partial Pt−Cl hydrolysis. Such a solvolysis is much more rapid in DMSO-d_6, where the signals of the C_{2v}-symmetrical **1** decline and the signals of the C_s-symmetrical **1′** arise in the course of 1−2 h (eq 1).

dx.doi.org/10.1021/ic402737f | Inorg. Chem. 2014, 53, 3371−3384

Table 2. Crystal Data for $(C_7H_{14}N_2)PtCl_2$ (1a), $(C_7H_{14}N_2)PtCl_2 \cdot Me_2NCHO$ (1b), $(C_7H_{14}N_2)PtCl_2 \cdot 3H_2O$ (1c), $(C_7H_{14}N_2)Pt\{C_4H_6(CO_2)_2\} \cdot 5H_2O$ (2b), and $(C_7H_{14}N_2)Pt(C_2O_4)$ (3)

	1a	1b	1c	2b	3
empirical formula	$C_7H_{14}Cl_2N_2Pt$	$C_{10}H_{21}Cl_2N_3OPt$	$C_7H_{20}Cl_2N_2O_3Pt$	$C_{13}H_{30}N_2O_9Pt$	$C_9H_{14}N_2O_4Pt$
color	colorless	colorless	yellow	colorless	colorless
formula wt	392.19	465.29	446.24	553.48	409.31
temp (K)	100	100	100	100	200
wavelength (Å)	0.71073	0.71073	0.71073	0.71073	0.71073
cryst syst	monoclinic	triclinic	orthorhombic	triclinic	triclinic
space group	$P2_1/n$ (No. 14)	$P\bar{1}$ (No. 2)	$Pnma$ (No. 62)	$P\bar{1}$ (No. 2)	$P\bar{1}$ (No. 2)
unit cell dimens					
a (Å)	11.7990(12)	6.4029(7)	11.5643(8)	9.4208(10)	7.0242(8)
b (Å)	7.0659(8)	6.7311(8)	12.4656(12)	12.9561(14)	7.8624(9)
c (Å)	12.1075(5)	16.8847(19)	8.8240(6)	16.9582(18)	10.0847(11)
α (deg)	90.0	91.573(2)	90.0	69.322(2)	94.5010(10)
β (deg)	91.753(6)	94.723(2)	90.0	88.402(2)	105.4650(10)
γ (deg)	90.0	92.842(2)	90.0	77.024(2)	99.2690(10)
V (Å^3)	1008.94(16)	723.98(14)	1272.03(17)	1884.1(3)	525.44(10)
Z	4	2	4	4	2
V/Z (Å^3)	252.2	362.0	318.0	471.0	262.7
calcd density (Mg m^{-3})	2.582	2.134	2.330	1.951	2.587
abs coeff (mm^{-1})	14.385	10.049	11.442	7.494	13.353
$F(000)$ (e)	728	444	848	1088	384
cryst size (mm^3)	0.20 × 0.16 × 0.08	0.03 × 0.02 × 0.02	0.38 × 0.28 × 0.06	0.38 × 0.21 × 0.20	0.04 × 0.04 × 0.02
θ range for data collecn (deg)	3.34−39.20	3.51−36.55	4.37−33.15	1.29−36.98	2.65−33.14
index ranges	$-20 \le h \le 20$	$-10 \le h \le 10$	$-17 \le h \le 17$	$-15 \le h \le 15$	$-10 \le h \le 10$
	$-12 \le k \le 12$	$-11 \le k \le 11$	$-19 \le k \le 19$	$-21 \le k \le 21$	$-12 \le k \le 12$
	$-21 \le l \le 21$	$-28 \le l \le 27$	$-13 \le l \le 13$	$-28 \le l \le 28$	$-15 \le l \le 15$
no. of rflns collected	43573	26539	30340	70909	13595
no. of indep rflns	5926 (R_{int} = 0.0279)	6699 (R_{int} = 0.0569)	2512 (R_{int} = 0.0252)	18024 (R_{int} = 0.0409)	3934 (R_{int} = 0.0383)
no. of rflns with $I > 2\sigma(I)$	5395	6318	2460	16135	3823
completeness (%)	99.8	99.3 (θ = 27.75°)	99.4 (θ = 33.15°)	100 (θ = 27.50°)	99.5 (θ = 27.50°)
abs cor	Gaussian	Gaussian	Gaussian	Gaussian	Gaussian
max/min transmissn	0.33/0.08	0.97/0.53	0.51/0.04	0.30/0.08	0.80/0.54
full-matrix least squares	F^2	F^2	F^2	F^2	F^2
no. of data/restraints/params	5926/0/109	6699/0/156	2512/4/87	18024/21/506	3934/0/145
goodness of fit on F^2	1.075	1.179	1.292	1.059	1.101
final R indices ($I > 2\sigma(I)$)					
R1	0.0171	0.0358	0.0118	0.0268	0.0243
wR2	0.0335	0.0958	0.0290	0.0671	0.0626
R indices (all data)					
R1	0.0208	0.0386	0.0125	0.0312	0.0252
wR2	0.0344	0.0969	0.0293	0.0690	0.0630
largest diff peak/hole (e Å^{-3})	1.201/−2.247	4.731/−4.394	0.651/−1.616	4.749/−2.091	1.946/−4.200

As for the spectra of **2** and **3** in DMSO-d_6, the signals of the bispidine ligand correspond to those of **1** in DMF-d_7, but the couplings are less resolved. Only the geminal coupling of NCH_eH_a1 is obvious, and for **2** the signals of NH and H_a1 are flanked by broad shoulders attributed to couplings $^{2,3}J$(PtH). For solutions of **2** and **3** in D_2O satellite couplings of H_a1 on the order of ^3J(PtH) = 76−77 Hz are also found, whereas the NH signal could not be detected here, presumably due to H/D exchange.

The ^{195}Pt NMR resonance[44,45] for **1** in CD_2Cl_2, DMF-d_7, and DMSO-d_6 was found at δ(Pt) −2240, which lies *between* the chemical shifts of *cis*-$(NH_3)_2PtCl_2$ (δ(Pt) −2077[40c]) and $(H_2NC_2H_4NH_2)PtCl_2$ (δ(Pt) −2345,[40a] −2323[40c]) (DMSO-d_6).

Molecular and Crystal Structures of $(C_7H_{14}N_2)PtCl_2$ (1a), $(C_7H_{14}N_2)PtCl_2 \cdot Me_2NCHO$ (1b), $(C_7H_{14}N_2)PtCl_2 \cdot 3H_2O$ (1c), $(C_7H_{14}N_2)Pt(C_2O_4C_4H_6) \cdot 5H_2O$ (2b), and $(C_7H_{14}N_2)Pt(C_2O_4)$ (3). The structures of **1a−c**, **2b**, and **3** have been determined by X-ray diffraction (Table 2). All compounds feature the same adamantane-type $(C_7H_{14}N_2)Pt$ skeleton. The Pt−N bonds are relatively short and are the shortest for complexes **2b** and **3** (2.021(2) Å, mean) containing carboxylate ligands, while they are slightly longer for complexes **1a−c** (2.035(6) Å) containing chloride as a coligand. All N−Pt−N angles are 85.6−86.6°, with larger N−Pt−N angles correlating with shorter Pt−N bonds for geometrical reasons. The nonbonding N···N distances are likewise relatively short at 2.76−2.78 Å, similar to the distance in the monoprotonated parent bispidine $[C_7H_{12}(NH)(NH_2)]Cl$ (cation i, 2.753 Å)[37] and much shorter than that for the ionic Pd complex $[(C_7H_{12}N_2allyl_2)Pd(\eta\text{-}C_3H_5)]PF_6$ (2.938 Å).[46] The dihedral angles C−C−N−C inside the piperidine six-membered rings are smaller (53.6−56.1°) than the ideal 60° and indicate some flattening of the chair conformation of the piperidine rings.

dx.doi.org/10.1021/ic402737f | Inorg. Chem. 2014, 53, 3371−3384

Nevertheless, the C−N−C and C−N−Pt angles at nitrogen (109.1−113.4°) are close to those of an ideal tetrahedron. All of the crystalline structures exhibit various modes of intermolecular N−H···Cl, C−H···Cl, and N−H···O hydrogen bonding.[47]

The solute-free **1a** (Figure 4a) crystallizes from methylformamide in the monoclinic crystal system, space group $P2_1/n$ (No. 14). The square-planar coordination geometry of the Pt atom is slightly distorted (dihedral angle N1,N2,Pt/Pt,Cl1,Cl2 = 2.9°). The compound forms pairs of equivalent molecules associated by 2-fold N1−H1···Cl1 bridges (N1···Cl1 = 3.243(1) Å), with the mean coordination planes of the two metal atoms being offset by 0.9 Å (Figure 4b). The halves of the complex pair are related to one another by an inversion center of symmetry at the center of the unit cell. The N−H···Cl bridges in the dimer are shorter than those found for other cisplatin-type complexes (see below), although they are markedly longer than the (acyclic) N−H···Cl bridges of the bis-HCl adduct of parent bispidine, $[C_7H_{12}(NH)_2Cl]Cl$ (3.055, 3.068 Å).[37] Contiguous dimers are approximately orientated perpendicular to one other, leading to a herringbone-type pattern when viewed along the *a* axis (Figure 4c). Association of the dimers to give the crystal seems based on weaker N2−H2···Cl2 (N2···Cl2 = 3.561(3) Å and 4.707(3) Å) and C−H···Cl interactions (e.g., C7···Cl1·= 3.548(3) Å). There is no stacking of the Pt centers in **1a**.

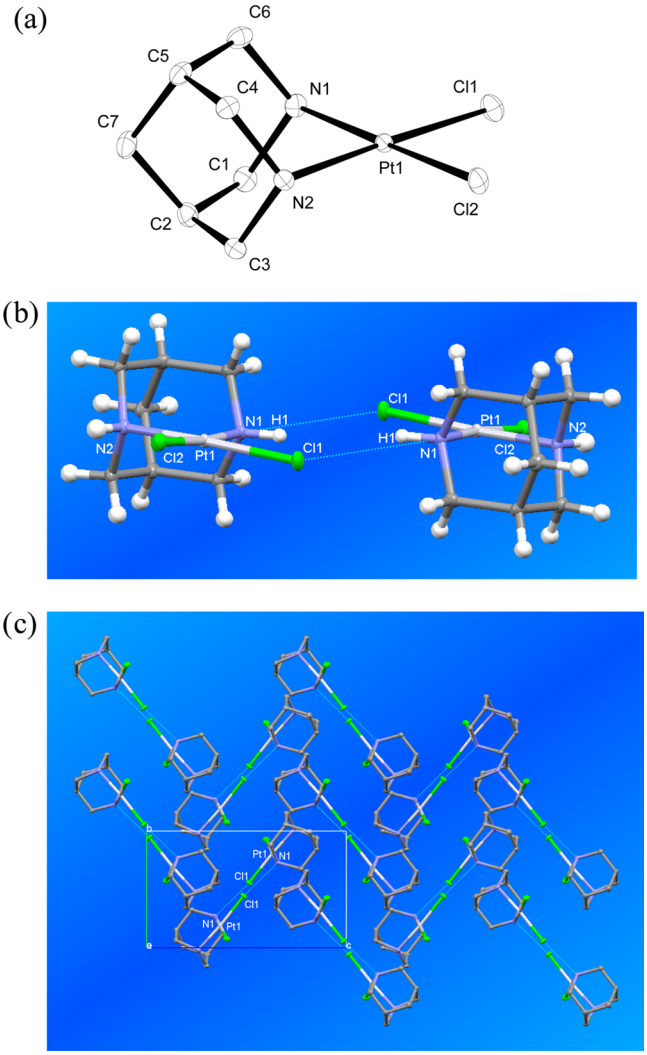

Figure 4. Crystal and molecular structure of $(C_7H_{14}N_2)PtCl_2$ (**1a**): (a) structure of the molecules; (b) dimeric unit; (c) association of the dimeric entities in a herringbone pattern (view along the *a* axis). Selected bond distances (Å), nonbonding distances (Å), and bond angles (deg): Pt1−N1 = 2.0413(14), Pt1−N2 = 2.0381(14), Pt−Cl1 = 2.3140(4), Pt−Cl2 = 2.3097(4), N1···N2 = 2.777(2), N1···Cl1 (intermolecular) = 3.243(1), N1−Pt1−N2 = 85.79(6), Cl1−Pt1−Cl2 = 92.212(15).

In DMF solute crystals of complex **1b** are obtained. The dimeric units of the complex are retained and solvated by a dimethylformamide molecule at both ends. The compound crystallizes in the triclinic crystal system in the space group $P\bar{1}$ (No. 2) with eight inversion centers in the unit cell. The solvation affects the dimeric units only slightly, inasmuch as the mean coordination planes of the Pt atoms in the complex pair are almost coplanar (offset of 0.15 Å, in comparison to 0.90 Å in **1a**) and the N1−H···Cl1 bridging distance (N1···Cl1 = 3.224(4) Å) is even slightly smaller than that in **1a** (Figure 5a).

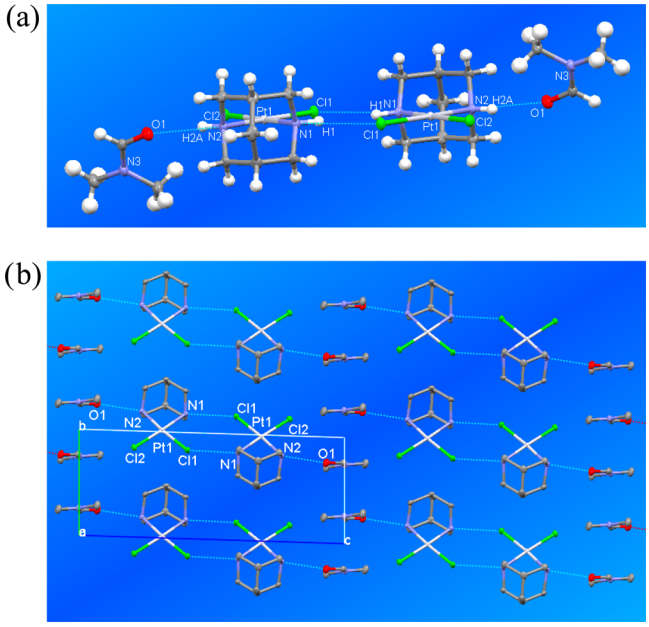

Figure 5. Molecular and crystal structure of $(C_7H_{14}N_2)PtCl_2 \cdot Me_2NCHO$ (**1b**): (a) structure of the dimeric unit; (b) packing of dimers in the crystal, viewed along the *a* axis showing the stacking of the dimethylformamide molecules. Selected bond distances (Å), nonbonding distances (Å), and bond angles (deg): Pt1−N1 = 2.037(4), Pt1−N2 = 2.029(4), Pt−Cl1 = 2.3224(12), Pt−Cl2 = 2.3226(11), N1···N2 = 2.772(6), N1···Cl1 (intermolecular) = 3.224(5), N2···O1 = 2.873(6), N1−Pt1−N2 = 85.99(16), Cl1−Pt1−Cl2 = 93.65(4).

The outer NH function of each bispidine ligand undergoes N2−H2···O1 hydrogen bonding to the carbonyl oxygen of a DMF molecule (N2···O1 = 2.873(6) Å); this bond appears to be among the shortest of this kind. The NC_3O plane of the DMF molecule lies 55° to the plane of the Pt complex. Even though N1 and N2 have different environments, the two Pt−N bonds are very similar in length (2.033(6) Å, mean); the same holds for Cl1 and Cl2 and the two Pt−Cl bonds (2.323(2) Å, mean). The packing of the solvated dimers in the crystal is such that strands of eclipsed dimers are interlaced with the neighboring strands via close stacking of the DMF molecules (Figure 5b). In agreement with the space group, both halves of

dx.doi.org/10.1021/ic402737f | Inorg. Chem. 2014, 53, 3371−3384

the solvated dimer, the neighboring strands of dimers, and contiguous DMF molecules are related to one another by centers of inversion. The Pt···Pt distance between parallel Pt coordination planes along the *b* axis corresponds to the unit cell dimension (6.7311(8) Å), excluding an interaction.

The structures of **1a,b** may be compared to those of cisplatin[7a,b] and derivatives[48] and various (ammine/amine)-$PtCl_2$–DMF cocrystals. Cisplatin forms two polymorphs which both occur in the space group $P\bar{1}$ and display stacks of planar molecules with alternating Pt···Pt distances of about 3.36–3.41 Å. Both polymorphs feature extended three-dimensional networks of N–H···Cl bonding with the shortest N···Cl distances of 3.27–3.42 Å.[7b] The solute compound *cis*-$(H_3N)_2PtCl_2$·DMF also forms two polymorphs, of which the orthorhombic form ($Pca2_1$) consists of layers of cisplatin and disordered DMF (N···O distances of 3.03 and 3.04 Å) in a nonstacking mode of the metal complexes.[7c] In the triclinic form ($P\bar{1}$) parallel square-planar Pt(II) complexes adhere pairwise to one another, supported by 4-fold N–H···Cl bonding (N···Cl = 3.389(7) and 3.403(7) Å), to form dimeric subunits with short Pt···Pt distances of 3.4071(7) Å, and these subunits are stacked upon another involving somewhat larger Pt···Pt distances (3.5534(8) Å).[7d] N···O distances of the cocrystals are 3.023(9) and 3.198(9) Å. Similar packing modes are also found for the complexes (1,2-DACH)$PtCl_2$·DMF (DMF bridges the NH functions with N···O = 2.971–3.039 Å),[18] (1,3-DACH)$PtCl_2$·DMF (containing a six-membered chelate ring as for **1a,b**; N···O = 2.893 Å),[49a] and (1,4-DACH)$PtCl_2$·DMF (N···O = 2.992 Å),[49b] which all form dimeric subunits with stacked parallel coordination planes, supported by 4-fold N–H···Cl hydrogen bonding (N···Cl = 3.31–3.52 Å), resulting in short Pt···Pt distances (3.336–3.519 Å). Taking into account that NH protons in an orientation perpendicular to the Pt plane are not required for the stacking of square-planar (diimine)PtX_2 complexes,[50] the absence of stacking with short Pt···Pt bonds indicates in the cases of **1a,b** that the bulk of the bispidine ligand promotes the formation of almost coplanar dimers.

Attempts to crystallize **1a,b** from water afforded the trihydrate **1c**, which crystallizes in the orthorhombic crystal system, space group *Pnma* (No. 62). Unexpectedly, the Pt complex in **1c** appears to exhibit no obvious interaction with the water. Instead, compound **1c** forms infinite parallel bands of bispidine–platinum dichloride complexes alternating in orientation and linked by two parallel N1–H···Cl1 bonds (N1···Cl1 = 3.250(2) Å) which are slightly longer than in **1a,b** (Figure 6). These bands stretching along the *b* axis are accompanied on both sides by zigzag-shaped strands of H-bonded water molecules (three molecules of water per complex entity). The coordination planes of adjacent Pt complexes are offset from each other by 0.44 Å. The complexes lie on planes of symmetry perpendicular to the coordination plane (which itself is not a mirror plane), passing through Pt1, C2, C3, and C4, and also O1 of one water molecule. Adjacent complex molecules are related by inversion.

The H-bonded water molecules follow the sequence ···O2···O1···O2*···O2···O1···O2*··· (O1···O2 = 2.743(2) Å and O2···O2* = 2.795(2) Å) such that O1 lies on the mirror plane and O2 and O2* are related by inversion, with hydrogen atoms disordered within the chain. The two chloride ions of a $PtCl_2$ moiety are symmetrically arranged about a proton of a water molecule, but the long Cl1···O1 distance of 3.415(2) Å indicates little if any interaction. The two adjacent water molecules, containing O2 and O2*, form slightly shorter contacts to the chloride ions of a $PtCl_2$ moiety of a neighboring chain (Cl1···O2 = 3.347(2) Å). Nevertheless, the band structure of the complex appears to be stabilized by this water network, since it does not exist without the water in either **1a** or **1b**.

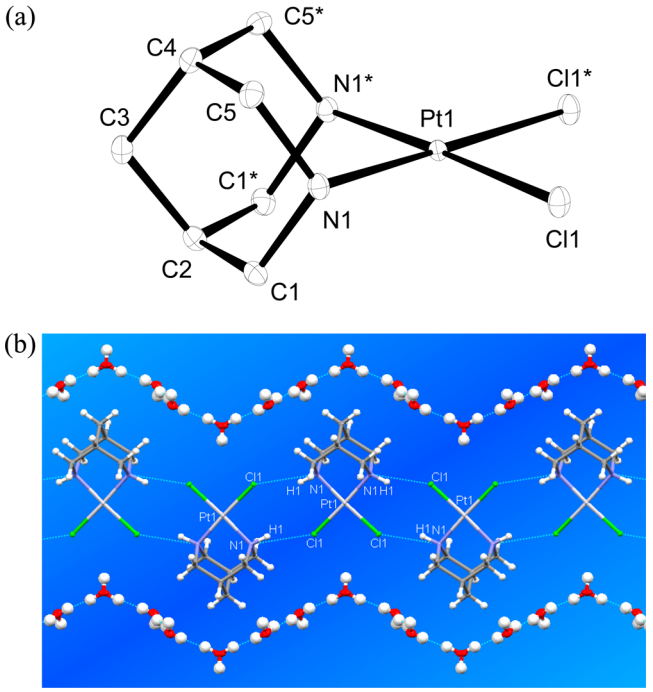

Figure 6. Crystal and molecular structure of $(C_7H_{14}N_2)PtCl_2·3H_2O$ (**1c**): (a) structure of the molecules; (b) association of the complex molecules including solute water (view along the *c* axis; H atoms in the hydrogen-bonded water chains are disordered over two positions and are present with half occupancy). Selected bond distances (Å), nonbonding distances (Å), and bond angles (deg): Pt1–N1 = 2.0289(12), Pt1–Cl1 = 2.3262(3), N1···N1* = 2.758(3), N1···Cl1 (intermolecular) = 3.250(2), N1–Pt1–N1* = 85.63(7), Cl1–Pt1–Cl1* = 91.114(17).

Compound **2b**, the bispidine analogue of carboplatin, crystallizes from water as the pentahydrate in the triclinic crystal system, space group $P\bar{1}$ (No. 2). The space group is the same as for **1b** and **3** and again exhibits 8 inversion centers in the unit cell. The asymmetric unit of crystalline **2b** contains 2 independent complex molecules, which are embedded in a 3-dimensional network of 10 inequivalent water molecules. While cisplatin analogues often crystallize from water with the inclusion of 1–3 solute water molecules (cf. **1c**), higher water contents are relatively rare. Two exceptions are $(H_3N)_2Pt$(nalidixate)·$5H_2O$,[51] which also contains 5 water molecules per complex, and the dinuclear Pt–methylenediphosphonate {(*cis*-1,2-DACH)Pt}$_2$(μ-$CH_2P_2O_6$)·$9H_2O$, which crystallizes as the nonahydrate.[19b]

The two independent complexes of **2b** in the unit cell are structurally very similar and differ mainly in the puckering of the Pt–dicarboxylate six-membered ring (torsion angles: Pt1–O2–C10–C9 = −13.8°; Pt2–O6–C23–C22 = 4.6°). Figure 7a shows the structure of one of the complexes. The coordination geometry at Pt, as defined by the Pt atom, the two N atoms of the bispidine, and two carboxylate O atoms of the malonic acid dicarboxylate ligand, is square planar (maximum deviation 0.04 Å). The Pt–dicarboxylate six-

dx.doi.org/10.1021/ic402737f | Inorg. Chem. 2014, 53, 3371–3384

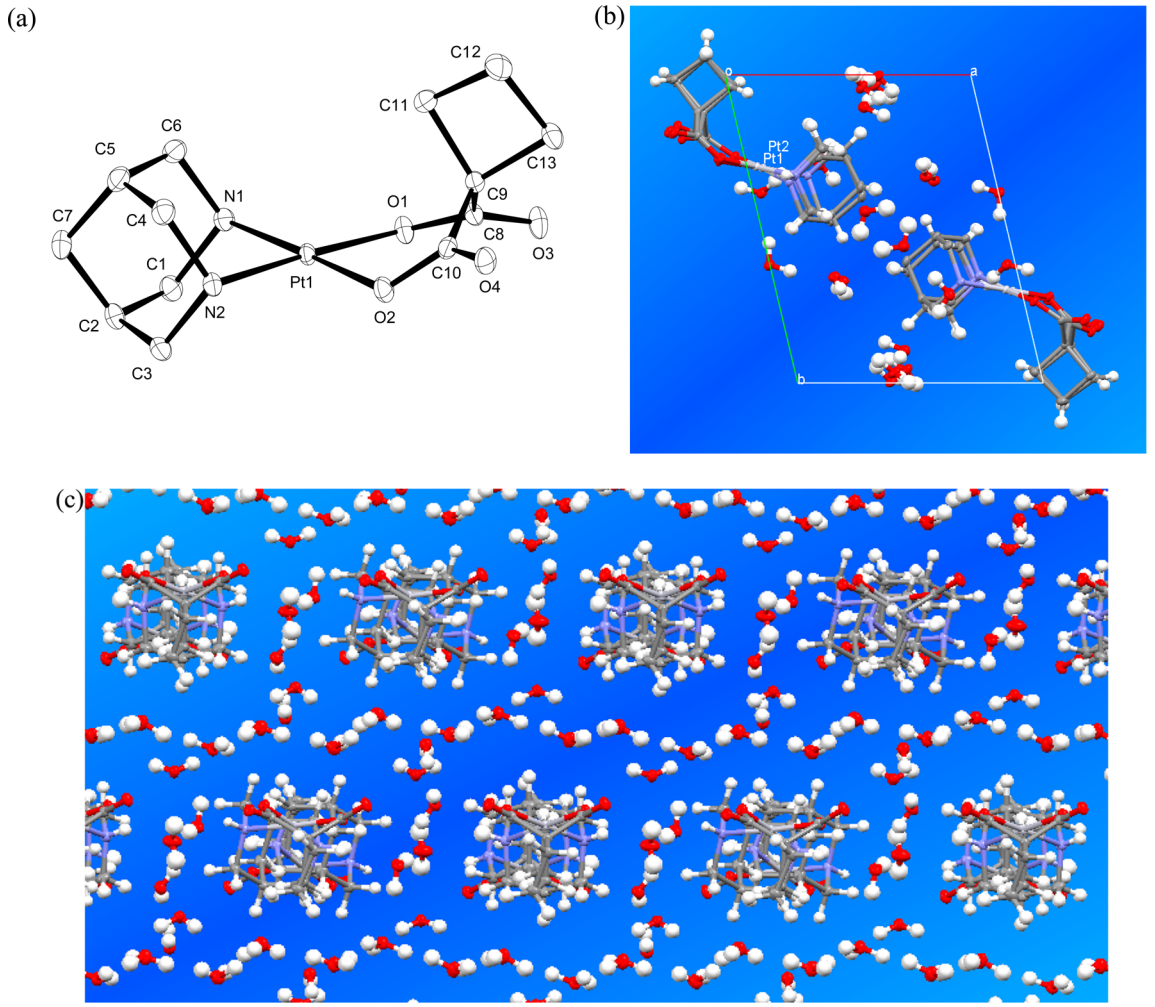

Figure 7. Crystal and molecular structure of $(C_7H_{14}N_2)Pt\{C_4H_6(CO_2)_2\}\cdot 5H_2O$ (**2b**): (a) drawing of the structure of molecule 1; (b) packing of molecules 1 and 2 viewed along the *c* axis; (c) slice through the packing of **2b**, showing the encapsulation of $(C_7H_{14}N_2)Pt\{C_4H_6(CO_2)_2\}$ molecules by water. Selected bond distances (Å), nonbonding distances (Å), and bond angles (deg): molecule 1, Pt1−N1 = 2.0218(17), Pt1−N2 = 2.0166(18), Pt1−O1 = 2.0375(16), Pt1−O2 = 2.0149(15), N1···N2 = 2.760(3), N1−Pt1−N2 = 86.21(7), O1−Pt1−O2 = 89.68(7); molecule 2, Pt2−N3 = 2.0192(18), Pt2−N4 = 2.0231(18), Pt2−O5 = 2.0211(16), Pt2−O6 = 2.0232(16), N3···N4 = 2.773(3), N3−Pt2−N4 = 86.63(8), O5−Pt2−O6 = 88.88(7).

membered rings in both molecules adopt a boat conformation, and the puckered cyclobutane rings, which lie almost perpendicular to the Pt coordination plane, are directed toward the opening of the boat, giving the molecules the curved structure that is typical for complexes of this ligand.[8b,c,10,11c] The Pt−N (2.020 Å, mean) and Pt−O distances (2.024 Å, mean) are all similar and are as expected.

Adjacent molecules 1 and 2 have similar orientations in the unit cell (Pt1 and Pt2 in Figure 7b). For both complex molecules the two N−H groups of the bispidine have N−H···O hydrogen bonds to the O atom of a water molecule (N···O(water) = 2.865(3)−2.938(3) Å). Additional C═O···H−O hydrogen bonding exists between the carbonyl functions of the malonate and water molecules (O(3,4,7,8)···O(water) = 2.748(3)−2.842(3) Å), whereas the carboxylate O atoms bonded to Pt do not appear to undergo any O···H−O hydrogen bond interactions to neighboring water molecules (O(1,2,5,6)···O(water) = 3.158(3)−3.805(3) Å). Both independent complexes are linked to one another by one water molecule (O10) that bridges the NH functions at N2 and N3 (on Pt1 and Pt2, respectively) and one water molecule (O18) that bridges the C═O functions at O4 and O7, forming a pair (Pt1···Pt2 = 8.024(1) Å). These pairs are linked by two further water molecules (O11 and O9), which are respectively bonded to the NH functions at N4 (on Pt2) and N1* (on Pt1*), and one water molecule (O13) that bridges the C═O functions at O8 and O3*; the corresponding longer Pt2···Pt1* distance is 8.941(1) Å. Thereby, along the *c* axis infinite chiral strands of alternating complex molecules Pt1···Pt2·····Pt1*···Pt2* separated by bridging water molecules are formed.

Extending in the direction of the *b* axis, each strand is joined by parallel inverted strands of sequence Pt1·····Pt2···Pt1*····· Pt2*. The closest approach between inverted molecules of adjacent strands is via their convex faces, resulting in nonbonding Pt···Pt distances of 4.703 Å (Pt1···Pt1**) and 4.784 Å (Pt2···Pt2**). For such "pairs" the cyclobutane rings at the peripheric concave faces mesh with those of the neighboring strand, and the corresponding Pt···Pt distances are here much larger (8.616−8.857 Å). The assembly of the parallel strands, including the water molecules, can be envisaged to form a layer of molecules extending in the *b*,*c* plane.

dx.doi.org/10.1021/ic402737f | *Inorg. Chem.* 2014, 53, 3371−3384

Such identical layers are piled up along the *a* axis. Therefore, along the *a* axis all molecules atop of one another are identical, and the molecules of adjoining reverse strands in consecutive layers are related by inversion (as is the case in the direction of the *b* axis). An assignment of the observed short-range structural effects of the eight inversion centers in the unit cell of **2b** is given in Table 3.

Table 3. Short-Range Structural Features of the Eight Inversion Centers in the Unit Cell of 2b

location of inversion center	short-range structural feature
origin	inversion of molecules Pt2 and Pt2* via their concave faces along *b* axis
a/2	O14···O14* inversion
b/2	inversion of molecules Pt2 and Pt2* via their convex faces along *b* axis
c/2	inversion of molecules Pt1 and Pt1* via their concave faces along *b* axis
midpoint of *ab* plane	inversion of diagonally opposite molecules Pt2 and Pt2* located in consecutive layers that pile up along *a* axis
midpoint of *ac* plane	O16···O16* inversion
midpoint of *bc* plane	inversion of molecules Pt1 and Pt1* via their convex faces along *b* axis
center of unit cell	inversion of diagonally opposite molecules Pt1 and Pt1* located in consecutive layers that pile up along *a* axis

Of the 10 independent water molecules of the framework, O9−O11 form N−H···O hydrogen bonds to the 4 NH groups (N1−N4) of the bispidine ligands as part of 7- and 8-membered-ring structures (Pt, N, C, and O), while O13−O18 form C═O···H−O hydrogen bonds to the four carbonyl groups (O3, O4, O7, and O8) of the dicarboxylate ligands as part of 9-membered-ring moieties (C and O). Only O12 is exclusively hydrogen bonded to other water molecules (O9, O13, and O18). Within the water framework (O(water)···O(water) = 2.676(3)−2.906(3) Å), 5-membered-ring structures of O atoms are the preferred structural motif. It is important to note that for **2b** all hydrogen-bonding interactions of the complex molecules involve the solute water; therefore, there are no direct hydrogen bonds between the complexes (Figure 7c).

Compound **3** can be considered as the bispidine analogue of oxaliplatin. It crystallizes from water in the triclinic crystal system, space group $P\bar{1}$ (No. 2), with two molecules of **3** in the unit cell and exclusion of water. Within the complexes (Figure 8a) the Pt−N bonds are very similar in length and relatively short (2.023(3) and 2.024(3) Å), as are the Pt−O bonds (2.026(2) and 2.028(2) Å). As expected for the oxalate ligand, the C−O bonds of the coordinating oxygen atoms are longer (1.291(4) and 1.306(3) Å) than the C═O bonds of the noncoordinating oxygen atoms (1.217(4) and 1.229(3) Å).

In the crystal, the complexes are aligned in parallel hydrogen-bonded chains (Figure 8b,c) along the $[1\bar{1}0]$ direction of the unit cell. The chains consist of alternating molecules that are orientated in opposite directions; adjacent molecules in the chain are related to one another by centers of inversion. Each two molecules appear to form dimeric and almost coplanar subunits (offset 0.28(1) Å; inversion center at *a*/2). Between contiguous subunits the offsets are larger (0.92(1) Å; inversion center at *b*/2).

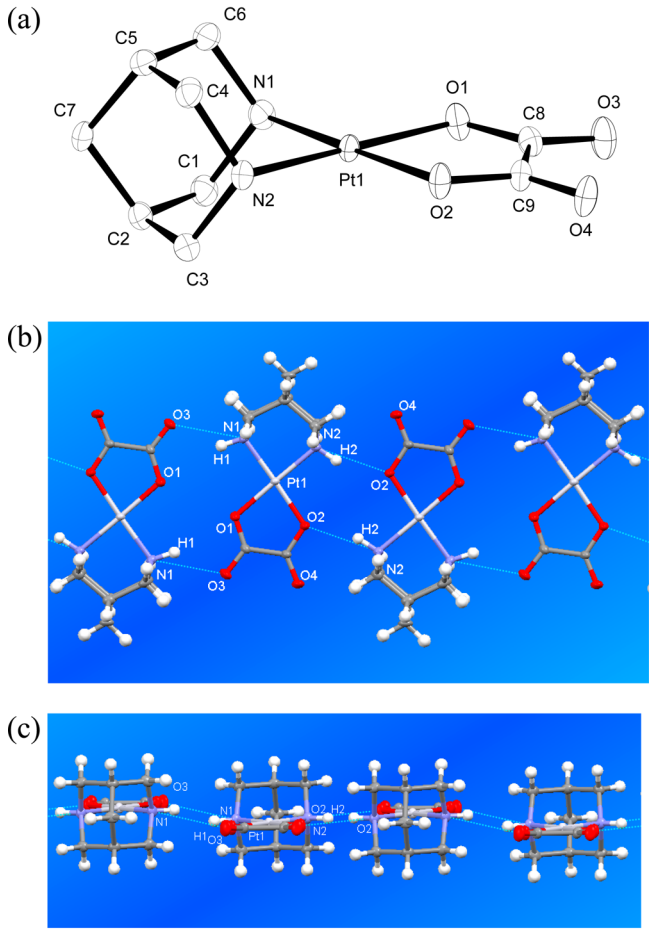

Figure 8. Crystal and molecular structure of $(C_7H_{14}N_2)Pt(C_2O_4)$ (**3**): (a) structure of the molecules; (b) association of the molecules by N1−H1···O3 and N2−H2···O2 bridge bonds (view perpendicular to the coordination plane of the metal); (c) as for (b), but viewed along the approximate 2-fold axes of the molecules. Selected bond distances (Å), nonbonding distances (Å), and bond angles (deg): Pt1−N1 = 2.024(3), Pt1−N2 = 2.023(3), Pt1−O1 = 2.026(2), Pt1−O2 = 2.028(2), N1···N2 = 2.758(4), N1···O3 (intermolecular) = 2.938(4), N2···O2 (intermolecular) = 2.976(4), N1−Pt1−N2 = 85.91(11), O1−Pt1−O2 = 82.62(10).

Linkage of the molecules in the chain occurs by two sets of parallel N−H···O bonds. Inside the nearly coplanar subunits the bonding is associated with a pair of N2−H2···O2 bonds (N2···O2 = 2.976(4) Å) between the bispidine ligand and one of the *coordinating* oxygen atoms of the neighboring oxalate; these bonds are relatively close to one another (the corresponding intramolecular N2···O2 distances are 3.012(4) Å). The subunits are connected by a pair of likewise parallel N1−H1···O3 bonds between the bispidine ligand and the *terminal* oxygen atom of the neighboring oxalate; these bonds are farther apart from one another (the intramolecular N1···O3 distances are 5.216(4) Å). The intermolecular N1···O3 distances between the subunits are 2.938(4) Å and are thus slightly shorter than the hydrogen-bonding interactions within the subunits (2.976(4) Å). This is consistent with the fact that the terminal oxygen atoms of carboxylate are expected to be more basic, and thus stronger "hydrogen bond acceptors",[52] than the metal-coordinating oxygen atoms (cf. **2b**, where only the terminal O atoms of the malonate form hydrogen bonds to water). All intermolecular N−H···O distances are significantly

dx.doi.org/10.1021/ic402737f | Inorg. Chem. 2014, 53, 3371−3384

longer than those involving the dimethylformamide ligand in **1b** (2.873(6) Å).

The packing of the parallel chains in the crystal is such that stacked planar complexes in different layers are related to one another by inversion centers at the origin (the Pt1···Pt1* distance is 5.203 Å) and the midpoint of the *ab* plane (Pt1···Pt1* is 4.892 Å) of the unit cell. Sideways neighboring molecules of adjacent chains within the same layer are related by inversions at the midpoints of the *ac* and *bc* planes and those of consecutive layers by inversions at *c*/2 and the center of the cell.

Since complex **3** crystallizes from aqueous solution with the total exclusion of water, in contrast to **2b**, it appears that the bispidine−oxalate N−H···O interactions are preferred over possible bispidine−water and oxalate−water interactions.

Cytotoxicity of Bispidine Analogues in Human Cancer Cell Lines. The cytotoxicities of cisplatin, carboplatin, and oxaliplatin and their bispidine analogues were determined with a functional MTT assay[53] in three human cancer cell lines: the ovarian cancer cell line A2780, their cisplatin-resistant subline A2780 CisR, and the human chronic myelogenous leukemia cell line K562. A2780 CisR is the cisplatin-resistant subline of the human ovarian carcinoma cell line A2780 and was generated by exposing the parental cell line to weekly cycles of cisplatin in an IC_{50} concentration[54] over a period of 24 weeks, as has been described before.[55] A2780 CisR shows a decreased sensitivity toward cisplatin, carboplatin, and oxaliplatin and serves together with the parental cell line as a model system to investigate the resistance against platinum-based chemotherapeutics. Furthermore, this model system can be used to identify compounds which can overcome the resistance.

As expected, carboplatin showed a reduced cytotoxic potency in comparison to cisplatin in all three cell lines, whereas oxaliplatin was more potent than cisplatin (Table 4).

Table 4. Cytotoxicity of Bispidine Analogues 1a, 2a, and 3 As Compared to Cisplatin, Carboplatin, and Oxaliplatin[a]

	pIC_{50}			
compd	A2780	A2780 CisR	K562	RF
cisplatin	5.86 ± 0.07	4.79 ± 0.04	4.92 ± 0.01	11.7
1a	5.38 ± 0.14	4.97 ± 0.18	~4.0[b]	2.52
carboplatin	5.37 ± 0.04	4.40 ± 0.06	4.14 ± 0.02	9.50
2a	5.05 ± 0.12	4.17 ± 0.14	~4.0[b]	6.46
oxaliplatin	6.66 ± 0.03	6.02 ± 0.12	5.25 ± 0.03	4.52
3	5.14 ± 0.17	4.45 ± 0.14	~3.6[b]	4.88

[a]Values are means ±SEM, each obtained from a representative experiment performed in triplicate. [b]Concentration inhibition curves did not reach bottom. The resistance factor (RF) was calculated as the ratio of the IC_{50} value of the A2780 CisR cells and the IC_{50} value of the corresponding sensitive parental A2780 cell line.

Furthermore, oxaliplatin exhibited a lower resistance factor (4.52) in the cisplatin resistance cell model A2780/A2780 CisR than either cisplatin or carboplatin (11.7 and 9.5, respectively), indicating full cross-resistance between cisplatin and carboplatin but reduced resistance against oxaliplatin.

Bispidine substitution in the three platinum complexes resulted in a decrease in cytotoxic potency, less so for the cisplatin and carboplatin analogues **1** and **2** and the most for the oxaliplatin analogue **3**, but the complexes still retained cytotoxic potency on the micromolar concentration level (Table 4). Interestingly, while compound **1a** was around 3-fold less potent at A2780 than cisplatin, it was slightly more cytotoxic against A2780 CisR. Thus, bispidine-substituted **1a** partially overcame resistance by reducing the resistance factor from 11.7 (cisplatin) to 2.52 (**1a**). Carboplatin and its bispidine analogue **2a** showed quite similar pIC_{50} values[54] in A2780 and A2780 CisR, respectively. However, **2a** reduced the resistance factor to a much lesser extent than the bispidine-substituted platinum compounds **1a** and **3**. To sum up, of the new Pt−bispidine complexes the cisplatin analogue **1a** appears to be most promising for further investigation, in particular with respect to overcoming the problem of platinum resistance.

CONCLUSIONS

We have described the synthesis, structure, and properties of three bispidine analogues of cisplatin, carboplatin, and oxaliplatin and investigated their cytotoxicity against three human cancer cell lines. The principal complexes are $(C_7H_{14}N_2)PtCl_2$ (**1a**), $(C_7H_{14}N_2)Pt\{C_4H_6(CO_2)_2\}$ (**2a**), and $(C_7H_{14}N_2)Pt(C_2O_4)$ (**3**), which are supplemented by a DMF solute (**1b**) and two hydrates (**1c**, **2b**).

Although the NH functional groups of bispidine should be less protic than those of ammonia or a primary amine, since bispidine is a secondary amine, the strong coordination of bispidine in the complexes **1**−**3** and concomitant electron transfer to Pt(II) appears to increase the NH protic character. As a result, **1**−**3** are able to form relatively strong (Pt)N−H···Cl and (Pt)N−H···O hydrogen bonds, by either self-association (**1a**, **2a**, and **3**) or coordination of basic solvent molecules, which serve as "hydrogen bond acceptors". The crystal structures illustrate how self-association and the interaction of the complexes with water and other solvent molecules may occur.

For the chloride, both the solute-free **1a** and the DMF solute **1b** are based on dimeric subunits. Whereas in the crystalline hydrate **1c** strings of water molecules appear to festoon and even stabilize the infinite strands of associated molecules of **1c**, this oligomeric association can be assumed to be relatively weak in the light of the dimeric subunits in **1a**,**b**. For the malonate, the complex molecules are completely encapsulated by water in the hydrate **2b**, whereas the oxalate **3** retains its oligomeric structure without incorporation of any water, even though it is crystallized from water. These results provide a plausible explanation why water solubility is highest for the malonate **2**, intermediate for the chloride **1**, and lowest for the oxalate **3**, since strong association between the complexes is expected to reduce solubility. In any case, water solubilities of **1**−**3** are at least comparable to those of their ammine congeners.

Complexes **1a**, **2a**, and **3** have been tested for their cytotoxicity against human cancer cell lines K562 (chronic myeloid leukemia), A2780, and A2780 CisR (ovarian cancer). Whereas all bispidine analogues showed significant cytotoxic activity in the micromolar range, bispidine substitution reduced the cytotoxic potency in comparison to their parent analogues except for **1a** at A2780 CisR. However, the bispidine-substituted compounds **1**−**3** partially overcame cisplatin resistance in A2780 CisR cells, as is evident from reduced resistance factors (Table 4). In an ongoing study we are investigating the effect of substitution of the bispidine ligand at the 9-position on the properties of these and related complexes.

dx.doi.org/10.1021/ic402737f | Inorg. Chem. 2014, 53, 3371−3384

EXPERIMENTAL SECTION

The reactions were performed under argon with Schlenk-type glassware. Syntheses of bispidine ($C_7H_{14}N_2$)[36g] and (1,5-hexadiene)-$PtCl_2$[38] were done according to the literature. 1,1-Cyclobutanedicarboxylic acid was obtained from Aldrich. NMR data of the products are given in Table 1. ^{195}Pt NMR spectra were recorded at 107.2 MHz, using an aqueous solution of K_2PtCl_6 (δ 0) as an external reference.

K_2(cbdca).[10e] An aqueous solution of 1,1-cyclobutanedicarboxylic acid (5.765 g, 40 mmol) was neutralized with 1 M KOH, as checked by pH test paper (pH 7). Evaporation of the water gave the product as a white powder: yield 8.80 g (quantitative); $C_6H_6K_2O_4$ (220.3).

Ag_2(cbdca).[10e] A solution of K_2(cbdca) (1100 mg, 5.00 mmol) in water (20 mL) was combined with an aqueous solution (20 mL) of $AgNO_3$ (1700 mg, 10.0 mmol). The product precipitated as a fine white powder, which was isolated by filtration, washed with cold H_2O (3 × 10 mL), and dried under vacuum: yield 1520 mg (85%); $C_6H_6Ag_2O_4$ (357.9). Exclusion of light is recommended.

($C_7H_{14}N_2$)$PtCl_2$ (1a). The reaction was performed as for **1b**, and the isolated crystalline solid was subjected to a vacuum at 50 °C for 24 h: yield 340 mg (87%) of solute-free **1a**. The amorphous compound can be recrystallized from *N*-methylformamide (50 °C) to afford pale yellow crystals of **1a**. According to DSC the compound is stable up to 280 °C. Anal. Calcd for $C_7H_{14}Cl_2N_2Pt$ (392.2): C, 21.44; H, 3.60; Cl, 18.08; N, 7.14; Pt, 49.74. Found: C, 21.49; H, 3.53; Cl, 18.08; N, 7.13; Pt, 49.68. IR: ν(NH) 3180 cm^{-1}. ESIpos MS (DMSO): *m*/*z* (%) 434 ([($C_7H_{14}N_2$)PtCl(DMSO)]$^+$, 100). ESIpos MS (H_2O): *m*/*z* (%) 414 ([M + Na]$^+$, 60), 747 ([2 M − Cl]$^+$, 100), 805 ([2 M + Na]$^+$, 40).

($C_7H_{14}N_2$)$PtCl_2$·C_3H_7NO (1b). When a light yellow solution of (C_6H_{10})$PtCl_2$ (348 mg, 1.00 mmol) and bispidine (126 mg, 1.00 mmol) in DMF (3 mL) was heated to 70 °C for 3 h, the color intensified. Slow recooling of the reaction solution to ambient temperature afforded large yellow cubes. These were freed from the mother liquor, washed with diethyl ether (−30 °C), and dried under vacuum: yield 405 mg (87%). The compound slowly eliminates DMF at ambient temperature under vacuum. Anal. Calcd for $C_{10}H_{21}Cl_2N_3OPt$ (465.3): C, 25.81; H, 4.55; Cl, 15.24; N, 9.03; O, 3.44; Pt, 41.93. Due to the ready elimination of solute molecules, no meaningful elemental analysis was obtainable.

($C_7H_{14}N_2$)$PtCl_2$·$3H_2O$ (1c). Compound **1a** (392 mg, 1.00 mmol), as a suspension in water (5 mL), was heated to 60 °C to obtain a yellow solution, concomitant with slight decomposition (Pt black deposition). After filtration the solution was slowly cooled to ambient temperature to afford pale yellow cuboids. These were washed with THF (0 °C) and dried under vacuum: yield 270 mg (60%). Anal. Calcd for $C_7H_{20}Cl_2N_2O_3Pt$ (446.2): C, 18.84; H, 4.52; Cl, 15.89; N, 6.28; O, 10.76; Pt, 43.72. Due to the ready elimination of solute molecules, no meaningful elemental analysis was obtainable.

($C_7H_{14}N_2$)Pt{$C_4H_6(CO_2)_2$} (2a). A suspension of ($C_7H_{14}N_2$)$PtCl_2$ (1.00 mmol, 392 mg) and Ag_2(cbdca) (1.00 mmol, 358 mg) in 40 mL of water was stirred at ambient temperature for 24 h. The precipitated AgCl was removed by filtration, and the clear solution was evaporated to dryness, eventually by heating to 50 °C, leaving a white powder: yield 440 mg (95%). Anal. Calcd for $C_{13}H_{20}N_2O_4Pt$ (463.4): C, 33.70; H, 4.35; N, 6.05; O, 13.81; Pt, 42.10. Found: C, 33.69; H, 4.34; N, 6.06; O, 13.81; Pt, 42.08. IR: ν(NH) 3136, ν(C=O) 1623, 1604, ν(C−O) 1360 cm^{-1}. ESIpos MS (H_2O): *m*/*z* (%) 486 ([M + Na]$^+$, 100), 949 ([2 M + Na]$^+$, 30). ESIpos MS (DMSO): *m*/*z* (%) 464 ([M + H]$^+$, 100), 486 ([M + Na]$^+$, 70), 927 ([2 M + H]$^+$, 30), 949 ([2 M + Na]$^+$, 20).

($C_7H_{14}N_2$)Pt{$C_4H_6(CO_2)_2$}·$5H_2O$ (2b). About 100 mg of **2a** was dissolved in 2 mL of water by heating to 70 °C. After recooling to ambient temperature colorless cubes of the pentahydrate **2b** separated after 1−2 days. Particularly large cubes of **2b** have been obtained by letting the water evaporate from a saturated aqueous solution of the complex, contained in a vessel open to the air, for 1−2 months. Such crystals, still moist, were used for the X-structure determination. Attempts to isolate the compound by drying under vacuum resulted in loss of water molecules. $C_{13}H_{30}N_2O_9Pt$ (553.5); no meaningful elemental analysis was obtainable.

($C_7H_{14}N_2$)Pt(C_2O_4) (3). A solution of ($C_7H_{14}N_2$)$PtCl_2$ (1.00 mmol, 392 mg) in 50 mL of water (50 °C) was treated with a solution of $AgNO_3$ (330 mg, 1.95 mmol) in 10 mL of water. Immediately, colorless AgCl precipitated, which after some further stirring (20 °C) was removed by filtration. $Na_2C_2O_4$ (130 mg, 0.97 mmol) was added, and the mixture was stirred overnight to afford an off-white precipitate, which was collected by filtration: yield 370 mg (90%). Recrystallization of the poorly soluble compound from hot water (70 °C) afforded thin colorless plates in lower yield (172 mg, 42%), owing to some hydrolysis. Anal. Calcd for $C_9H_{14}N_2O_4Pt$ (409.3): C, 26.41; H, 3.45; N, 6.84; O, 15.64; Pt, 47.66. Found: C, 26.23; H, 3.41; N, 6.75; Pt, 47.12. IR: ν(NH) 3161, ν(C=O) 1697, 1659, ν(C−O) 1378 cm^{-1}. ESIpos MS (H_2O): *m*/*z* (%) 409 ([M + Na]$^+$, 40), 841 ([2 M + Na]$^+$, 100). ESIpos MS (DMSO): *m*/*z* (%) 410 ([M + H]$^+$, 80), 432 ([M + Na]$^+$, 100), 819 ([2 M + H]$^+$, 20), 841 ([2 M + Na]$^+$, 40).

Biological Studies. Cell Lines, and Cell Culture. The human ovarian carcinoma cell line A2780 was obtained from the European Collection of Cell Cultures (ECACC, Salisbury, U.K.). The cisplatin-resistant subline A2780 CisR was established by exposure to weekly cycles of 2 μmol/L cisplatin over a period of 24 weeks.[55] The human chronic myelogenous leukemia cell line K562 was obtained from the German Collection of Microorganisms and Cell Cultures (DSMZ, Germany).

All cell lines were grown at 37 °C under humidified air supplemented with 5% CO_2 in RPMI 1640 (PAN Biotech, Germany) containing 10% heat-inactivated fetal bovine serum (PAN Biotech, Germany), 100 IU/mL of penicillin (Sigma, Germany), and 100 μg/mL of streptomycin (Sigma, Germany). The cells were grown to 80% confluence before using them for the MTT cell viability assay.

Stock solutions for cisplatin were made by dissolving cisplatin in sodium chloride to a final concentration of 5 mM, whereas glucose 5% was used for preparing the stock solutions for carboplatin (5 mM) and oxaliplatin (3.16 mM). Compounds **1a**, **2a**, and **3** were dissolved in distilled water to a final concentration of 10 mM. Serial dilutions of all compounds were prepared in sodium chloride 0.9%.

MTT Cell Viability Assays. The rate of cell survival under the action of test compounds was evaluated by an improved MTT assay as previously described.[53] The assay is based on the ability of viable cells to metabolize yellow 3-(4,5-dimethylthiazol-2-yl)-2,5-diphenyltetrazolium bromide (MTT, Applichem, Germany) to violet formazane crystals that can be detected spectrophotometrically. In brief, A2780 and A2780 CisR cells were seeded at a density of 8000 cells/well and K562 at a density of 30000 cells/well in 96-well plates (Corning, Germany) in 90 μL of drug-free complete medium. After 24 h, cells were exposed to dilutions of the test compounds in 100 μL/well. Incubation was ended after 72 h, and cell survival was determined by addition of 25 μL/well MTT solution (5 mg/mL in phosphate-buffered saline). Absorbance was measured at 544 and 690 nm with a FLUOstar microplate reader (BMG LabTech, Offenburg, Germany). The absorbance of untreated control cells was taken as 100% viability. All tests were performed in triplicate.

Data Analysis. Indicated are mean values ± standard error of the mean. Concentration/effect curves were fitted to the data by nonlinear regression analysis using the four-parameter logistic equation (GraphPad Prism).

ASSOCIATED CONTENT

Supporting Information

Figures giving IR spectra of compounds **1**−**3** and CIF files giving crystallographic data for **1a**−**c**, **2b**, and **3**. This material is available free of charge via the Internet at http://pubs.acs.org.

AUTHOR INFORMATION

Corresponding Author

*E-mail for K.-R.P.: poerschke@kofo.mpg.de.

Author Contributions

All authors contributed to the writing of this manuscript.

Notes

The authors declare no competing financial interest.

■ ACKNOWLEDGMENTS

We thank members of the analytical departments for their help with this project, in particular Angelika Dreier and Jörg Rust from chemical crystallography and Dr. Christophe Farès from NMR spectroscopy.

■ REFERENCES

(1) (a) Peyrone, M. *Ann. Chem. Pharm.* **1844**, *51*, 1. (b) Lippard, S. J. *Science* **1982**, *218*, 1075. (c) Kauffman, G. B.; Pentimalli, R.; Doldi, S.; Hall, M. D. *Platinum Met. Rev.* **2010**, *54*, 250.

(2) (a) Rosenberg, B.; Van Camp, L.; Krigas, T. *Nature* **1965**, *205*, 698. (b) Rosenberg, B.; Van Camp, L.; Trosko, J. E.; Mansour, V. H. *Nature* **1969**, *222*, 385. (c) Rosenberg, B.; Van Camp, L. *Cancer Res.* **1970**, *30*, 1799. (d) Rosenberg, B. *Platinum Met. Rev.* **1971**, *15*, 42. (e) Rosenberg, B. *Interdiscip. Sci. Rep.* **1978**, *3*, 134. (f) Rosenberg, B. In *Nucleic Acid–Metal Ion Interactions*; Spiro, T. G., Ed.; Wiley: New York, 1980; pp 1–29.

(3) (a) *Cisplatin*; Lippert, B., Ed.; Wiley-VCH: Weinheim, Germany, 1999. (b) Alderden, R. A.; Hall, M. D.; Hambley, T. W. *J. Chem. Educ.* **2006**, *83*, 728. (c) *The Discovery, Use and Impact of Platinum Salts as Chemotherapy Agents for Cancer*; Christie, D. A., Tansey, E. M., Eds.; Wellcome Trust Centre for the History of Medicine at UCL: London, 2007; Wellcome Witnesses to Twentieth Century Medicine Series Vol. *30*, ISBN 978-085484-112-7.

(4) (a) *Platinum-based drugs in cancer therapy*; Kelland, L. R., Farrell, N. P., Eds.; Humana (Springer): New York, 2000, reprinted 2010. (b) Jakupec, M. A.; Galanski, M.; Keppler, B. K. *Rev. Physiol. Biochem. Pharmacol.* **2003**, *146*, 1. (c) *Metal Compounds in Cancer Chemotherapy*; Pérez, J. M., Fuertes, M. A., Alonso, C., Eds.; Research Signpost: Trivandrum, India, 2005. (d) *Platinum and Other Heavy Metal Compounds in Cancer Chemotherapy*; Bonetti, A., Leone, R., Muggia, F. M., Howell, S. B., Eds.; Humana (Springer): New York, 2009.

(5) (a) Highley, M. S.; Calvert, A. H. Clinical Experience with Cisplatin and Carboplatin. In ref 4a, p 171. (b) Vaughan, M.; Sapunar, F.; Gore, M. Clinical Experience. Platinum and Taxanes. In ref 4a, p 195. (c) O'Dwyer, P. J.; Stevenson, J. P.; Johnson, S. W. Clinical Experience. DACH-Based Platinum Drugs. In ref 4a, p 231. (d) McKeage, M. J. Clinical Toxicology of Platinum-Based Cancer Chemotherapeutic Agents. In ref 4a, p 251.

(6) (a) Wiltshaw, E. *Platinum Met. Rev.* **1979**, *23*, 90. (b) Barnard, C. F. J. *Platinum Met. Rev.* **1989**, *33*, 162.

(7) (a) Milburn, G. H. W.; Truter, M. R. *J. Chem. Soc. A* **1966**, 1609. (b) Ting, V. P.; Schmidtmann, M.; Wilson, C. C.; Weller, M. T. *Angew. Chem., Int. Ed.* **2010**, *49*, 9408. (c) Raudaschl, G.; Lippert, B.; Hoeschele, J. D.; Howard-Lock, H. E.; Lock, C. J. L.; Pilon, P. *Inorg. Chim. Acta* **1985**, *106*, 141. (d) Johnston, D. H.; Miller, N. A.; Tackett, C. B. *Acta Crystallogr., Sect. E: Struct. Rep. Online* **2012**, *68*, m863. (e) Raudaschl-Sieber, G.; Lippert, B.; Britten, J. F.; Beauchamp, A. L. *Inorg. Chim. Acta* **1986**, *124*, 213. (f) Alston, D. R.; Stoddart, J. F.; Williams, D. J. *J. Chem. Soc., Chem. Commun.* **1985**, 532.

(8) (a) Harrison, R. C.; McAuliffe, C. A.; Zaki, A. M. *Inorg. Chim. Acta* **1980**, *46*, L15. (b) Neidle, S.; Ismail, I. M.; Sadler, P. J. *J. Inorg. Biochem.* **1980**, *13*, 205. (c) Beagley, B.; Cruickshank, D. W. J.; McAuliffe, C. A.; Pritchard, R. G.; Zaki, A. M.; Beddoes, R. L.; Cernik, R. J.; Mills, O. S. *J. Mol. Struct.* **1985**, *130*, 97.

(9) Harrap, K. R. *Cancer Treat. Rev. (Suppl. A)* **1985**, *12*, 21.

(10) (a) Bitha, P.; Morton, G. O.; Dunne, T. S.; Delos Santos, E. F.; Lin, Y.; Boone, S. R.; Haltiwanger, R. C.; Pierpont, C. G. *Inorg. Chem.* **1990**, *29*, 645. (b) Guo, Z.; Habtemariam, A.; Sadler, P. J.; Palmer, R.; Potter, B. S. *New J. Chem.* **1998**, 11. (c) Rochon, F. D.; Gruia, L. M. *Inorg. Chim. Acta* **2000**, *306*, 193. (d) Alvarez-Valdés, A.; Pérez, J. M.; López-Solera, I.; Lannegrand, R.; Continente, J. M.; Amo-Ochoa, P.; Camazón, M. J.; Solans, X.; Font-Bardía, M.; Navarro-Ranninger, C. *J. Med. Chem.* **2002**, *45*, 1835. (e) Rochon, F. D.; Massarweh, G. *Inorg. Chim. Acta* **2006**, *359*, 4095.

(11) (a) Barnes, J. C.; Iball, J.; Weakley, T. J. R. *Acta Crystallogr., Sect. B: Struct. Crystallogr. Cryst. Chem.* **1975**, *31*, 1435. (b) Khan, S. R. A.; Guzman-Jimenez, I.; Whitmire, K. H.; Khokhar, A. R. *Polyhedron* **2000**, *19*, 983. (c) Ali, M. S.; Thurston, J. H.; Whitmire, K. H.; Khokhar, A. R. *Polyhedron* **2002**, *21*, 2659. (d) Mukhopadhyay, U.; Thurston, J. H.; Whitmire, K. H.; Khokhar, A. R. *Polyhedron* **2002**, *21*, 2369.

(12) (a) van Kralingen, C. G.; Reedijk, J.; Spek, A. L. *Inorg. Chem.* **1980**, *19*, 1481. (b) Cutbush, S. D.; Kuroda, R.; Neidle, S.; Robins, A. B. *J. Inorg. Biochem.* **1983**, *18*, 213. (c) Brown, B. E.; Lock, C. J. L. *Acta Crystallogr., Sect. C: Cryst. Struct. Commun.* **1989**, *45*, 993. (d) Bitha, P.; Carvajal, S. G.; Citarella, R. V.; Child, R. G.; Delos Santos, E. F.; Dunne, T. S.; Durr, F. E.; Hlavka, J. J.; Lang, S. A., Jr.; Lindsay, H. L.; Morton, G. O.; Thomas, J. P.; Wallace, R. E.; Lin, Y.; Haltiwanger, R. C.; Pierpont, C. G. *J. Med. Chem.* **1989**, *32*, 2015. (e) Cho, S. W.; Cho, Y.; Kim, D.-K.; Shin, W. *Acta Crystallogr., Sect. C: Cryst. Struct. Commun* **2000**, *56*, 653. (f) Chekhlov, A. N. *Russ. J. Inorg. Chem.* **2004**, *49*, 1866.

(13) Rochon, F. D.; Melanson, R.; Macquet, J.-P.; Belanger-Gariepy, F.; Beauchamp, A. L. *Inorg. Chim. Acta* **1985**, *108*, 1.

(14) Galanski, M.; Jakupec, M. A.; Keppler, B. K. Oxaliplatin and derivatives as anticancer drugs–novel design strategies. In ref 4c, p 155.

(15) Kidani, Y.; Noji, M.; Tashiro, T. *Gann* **1980**, *71*, 637.

(16) Habala, L.; Galanski, M.; Yasemi, A.; Nazarov, A. A.; von Keyserlingk, N. G.; Keppler, B. K. *Eur. J. Med. Chem.* **2005**, *40*, 1149.

(17) (a) Bruck, M. A.; Bau, R.; Noji, M.; Inagaki, K.; Kidani, Y. *Inorg. Chim. Acta* **1984**, *92*, 279. (b) Abu-Surrah, A. S.; Al-Allaf, T. A. K.; Klinga, M.; Ahlgren, M. *Polyhedron* **2003**, *22*, 1529.

(18) Spingler, B.; Whittington, D. A.; Lippard, S. J. *Inorg. Chem.* **2001**, *40*, 5596.

(19) (a) Rochon, F. D.; Melanson, R.; Macquet, J.-P.; Belanger-Gariepy, F.; Beauchamp, A. L. *Inorg. Chim. Acta* **1985**, *108*, 17. (b) Bau, R.; Huang, S. K. S.; Feng, J.-A.; McKenna, C. E. *J. Am. Chem. Soc.* **1988**, *110*, 7546. (c) Miyamoto, T. K.; Okude, K.; Maeda, K.; Ichida, H.; Sasaki, Y.; Tashiro, T. *Bull. Chem. Soc. Jpn.* **1989**, *62*, 3239. (d) Okude, K.; Ichida, H.; Miyamoto, T. K.; Sasaki, Y. *Acta Crystallogr., Sect. C: Cryst. Struct. Commun.* **1989**, *45*, 949. Miyamoto, T. K.; Ichida, H. *Bull. Chem. Soc. Jpn.* **1991**, *64*, 1835. (e) Miyamoto, T. K.; Ichida, H. *Chem. Lett.* **1991**, 435. (f) Hata, G.; Kitano, Y.; Kaneko, T.; Kawai, H.; Mutoh, M. *Chem. Pharm. Bull.* **1992**, *40*, 1604. (g) Yuge, H.; Miyamoto, T. K. *Acta Crystallogr., Sect. C: Cryst. Struct. Commun.* **1997**, *53*, 1816. (h) Carland, M.; Tan, K. J.; White, J. M.; Stephenson, J.; Murray, V.; Denny, W. A.; McFadyen, W. D. *J. Inorg. Biochem.* **2005**, *99*, 1738.

(20) (a) Battle, A. R.; Deacon, G. B.; Dolman, R. C.; Hambley, T. W. *Aust. J. Chem.* **2002**, *55*, 699. (b) Al-Allaf, T. A. K.; Rashan, L. J.; Steinborn, D.; Merzweiler, K.; Wagner, C. *Transition Met. Chem.* **2003**, *28*, 717. (c) Galanski, M.; Yasemi, A.; Slaby, S.; Jakupec, M. A.; Arion, V. B.; Rausch, M.; Nazarov, A. A.; Keppler, B. K. *Eur. J. Med. Chem.* **2004**, *39*, 707.

(21) (a) Sherman, S. E.; Lippard, S. J. *Chem. Rev.* **1987**, *87*, 1153. (b) Reedijk, J. *Chem. Commun.* **1996**, 801. (c) Jamieson, E. R.; Lippard, S. J. *Chem. Rev.* **1999**, *99*, 2467. (d) Wang, D.; Lippard, S. J. *Nat. Rev.* **2005**, *4*, 307. (e) Jung, Y.; Lippard, S. J. *Chem. Rev.* **2007**, *107*, 1387. (f) Arnesano, F.; Natile, G. *Coord. Chem. Rev.* **2009**, *253*, 2070. (g) Gibson, D. *Dalton Trans.* **2009**, 10681. (h) Klein, A. V.; Hambley, T. W. *Chem. Rev.* **2009**, *109*, 4911.

(22) (a) Gately, D. P.; Howell, S. B. *Br. J. Cancer* **1993**, *67*, 1171. (b) Andrews, P. A. Cisplatin accumulation. In ref 4a, p 89. (c) Hall, M. D.; Okabe, M.; Shen, D.-W.; Liang, X.-J.; Gottesman, M. M. *Annu. Rev. Pharmacol. Toxicol.* **2008**, *48*, 495. (d) Olszewski, U.; Hamilton, G. *Anti-Cancer Agents Med. Chem.* **2010**, *10*, 293.

(23) Herman, F.; Kozelka, J.; Stoven, V.; Guittet, E.; Girault, J.-P.; Huynh-Dinh, T.; Igolen, J.; Lallemand, J.-Y.; Chottard, J.-C. *Eur. J. Biochem.* **1990**, *194*, 119.

(24) (a) Johnson, S. W.; Ferry, K. V.; Hamilton, T. C. *Drug Res. Updates* **1998**, *1*, 243. (b) Brabec, V. Chemistry and Structural Biology

of 1,2-Interstrand Adducts of Cisplatin. In ref 4a, p 37. (c) Brown, R. Cisplatin Resistance in Ovarian Cancer. In ref 4a, p 115. (d) Fink, D.; Howell, S. B. How Does Cisplatin Kill Cells? In ref 4a, p 149. (e) Shen, D.-W.; Pouliot, L. M.; Hall, M. D.; Gottesman, M. M. *Pharmacol. Rev.* **2012**, *64*, 706.

(25) (a) van Zutphen, S.; Reedijk, J. *Coord. Chem. Rev.* **2005**, *249*, 2845. (b) Reedijk, J. *Eur. J. Inorg. Chem.* **2009**, 1303. (c) Lovejoy, K. S.; Lippard, S. J. *Dalton Trans.* **2009**, 10651.

(26) (a) Cleare, M. J.; Hoeschele, J. D. *Bioinorg. Chem.* **1973**, *2*, 187. (b) Cleare, M. J.; Hoeschele, J. D. *Platinum Met. Rev.* **1973**, *17*, 2. (c) Cleare, M. J. *Coord. Chem. Rev.* **1974**, *12*, 349. (d) Cleare, M. J. *J. Clin. Hematol. Oncol.* **1977**, *7*, 1. (e) Connors, T. A.; Cleare, M. J.; Harrap, K. R. *Cancer Treat. Rep.* **1979**, *63*, 1499. (f) van der Veer, J. L.; Reedijk, J. *Chem. Br.* **1988**, *24*, 775. (g) de Mier-Vinué, J.; Montaña, A. M.; Moreno, V. Platinum complexes with cytotoxic activity: Models for structure−activity relationship studies. In ref 4c, p 47. (h) Montaña, A. M.; Batalla, C. *Curr. Med. Chem.* **2009**, *16*, 2235.

(27) (a) Reedijk, J. *Inorg. Chim. Acta* **1992**, *198*, 873. (b) Reedijk, J. *Platinum Met. Rev.* **2008**, *52*, 2. (c) Miguel, P. J. S.; Roitzsch, M.; Yin, L.; Lax, P. M.; Holland, L.; Krizanovic, O.; Lutterbeck, M.; Schürmann, M.; Fusch, E. C.; Lippert, B. *Dalton Trans.* **2009**, 10774.

(28) (a) Rochon, F. D.; Melanson, R. *Inorg. Chem.* **1987**, *26*, 989. (b) Fanizzi, F. P.; Maresca, L.; Natile, G.; Lanfranchi, M.; Manotti-Lanfredi, A. M.; Tiripicchio, A. *Inorg. Chem.* **1988**, *27*, 2422. (c) Xu, Q.; Khokhar, A. R.; Bear, J. L. *Inorg. Chim. Acta* **1990**, *178*, 107. (d) Rezler, E. M.; Fenton, R. R.; Esdale, W. J.; McKeage, M. J.; Russell, P. J.; Hambley, T. W. *J. Med. Chem.* **1997**, *40*, 3508. (e) Mullaney, M.; Chang, S.-C.; Norman, R. E. *Inorg. Chim. Acta* **1997**, *265*, 275. (f) Galanski, M.; Berger, M.; Keppler, B. K. *Met.-Based Drugs* **2000**, *7*, 349. (g) Intini, F. P.; Cini, R.; Tamasi, G.; Hursthouse, M. B.; Natile, G. *Inorg. Chem.* **2008**, *47*, 4909. (h) Luzyanin, K. V.; Gushchin, P. V.; Pombeiro, A. J. L.; Haukka, M.; Ovcharenko, V. I.; Kukushkin, V. Y. *Inorg. Chem.* **2008**, *47*, 6919.

(29) (a) Kimura, E.; Korenari, S.; Shionoya, M.; Shiro, M. *J. Chem. Soc., Chem. Commun.* **1988**, 1166. (b) Ling, E. C. H.; Allen, G. W.; Hambley, T. W. *J. Am. Chem. Soc.* **1994**, *116*, 2673. Allen, G. W.; Ling, E. C. H.; Krippner, L. V.; Hambley, T. W. *Aust. J. Chem.* **1996**, *49*, 1301. (c) Teo, C.-L.; Fenton, R. R.; Turner, P.; Hambley, T. W. *Aust. J. Chem.* **1998**, *51*, 977. (d) Munk, V. P.; Fenton, R. R.; Hambley, T. W. *Polyhedron* **1999**, *18*, 1039. (e) Davies, M. S.; Fenton, R. R.; Huq, F.; Ling, E. C. H.; Hambley, T. W. *Aust. J. Chem.* **2000**, *53*, 451. (f) Ali, M. S.; Powers, C. A.; Whitmire, K. H.; Guzman-Jimenez, I.; Khokhar, A. R. *J. Coord. Chem.* **2001**, *52*, 273.

(30) (a) For $(C_4H_8N_2Me_2)PtCl_2$, see: Ciccarese, A.; Clemente, D. A.; Fanizzi, F. P.; Marzotto, A.; Valle, G. *Inorg. Chim. Acta* **1998**, *275*−*276*, 410. (b) Attempts to synthesize $(C_4H_{10}N_2)PtCl_2$ resulted in the formation of the dinuclear complex $(\mu\text{-}C_4H_{10}N_2)_2(PtCl_2)_2$[30c] or $[(C_4H_{10}N_2)_2Pt][PtCl_4]_2$.[30d] (c) Kukushkin, Y.; Yurinov, V. A. *Zh. Neorg. Khim.* **1971**, *16*, 1134. (d) Ivanova, N. A.; Kurbakova, A. P.; Efimenko, I. A. *Koord. Khim.* **1993**, *19*, 911.

(31) Robertazzi, A.; Platts, J. A. *J. Comput. Chem.* **2004**, *25*, 1060.

(32) Michael, J. P. *Nat. Prod. Rep.* **2008**, *25*, 139 and previous reviews.

(33) (a) Jeyaraman, R.; Avila, S. *Chem. Rev.* **1981**, *81*, 149. (b) Zefirov, N. S.; Palyulin, V. A. *Top. Stereochem.* **1991**, *20*, 171. (c) Comba, P.; Kerscher, M.; Schiek, W. *Prog. Inorg. Chem.* **2007**, *55*, 613. (d) Hancock, R. D.; Melton, D. L.; Harrington, J. M.; McDonald, F. C.; Gephart, R. T.; Boone, L. L.; Jones, S. B.; Dean, N. E.; Whitehead, J. R.; Cockrell, G. M. *Coord. Chem. Rev.* **2007**, *251*, 1678. (e) Breuning, M.; Steiner, M. *Synthesis* **2008**, *18*, 2841.

(34) Black, D. S. C.; Deacon, G. B.; Rose, M. *Tetrahedron* **1995**, *51*, 2055.

(35) Stetter, H.; Merten, R. *Chem. Ber.* **1957**, *90*, 868.

(36) (a) Bohlmann, F.; Ottawa, N.; Keller, R. *Liebigs Ann. Chem.* **1954**, *587*, 162. (b) Bohlmann, F.; Ottawa, N. *Chem. Ber.* **1955**, *88*, 1828. (c) Galinovsky, F.; Langer, H. *Monatsh. Chem.* **1955**, *86*, 449. (d) Galinovsky, F.; Sparatore, F.; Langer, H. *Monatsh. Chem.* **1956**, *87*, 100. (e) Stetter, H.; Hennig, H. *Chem. Ber.* **1955**, *88*, 789. (f) Stetter, H.; Merten, R. *Chem. Ber.* **1957**, *90*, 868. (g) Miyahara, Y.; Goto, K.; Inazu, T. *Synthesis* **2001**, 364.

(37) Cui, H.; Goddard, R.; Pörschke, K.-R. *J. Phys. Org. Chem.* **2012**, *25*, 814.

(38) (a) Jensen, K. A. *Acta Chem. Scand.* **1953**, *7*, 866. (b) Garcia, L.; Shupack, S. I.; Orchin, M. *Inorg. Chem.* **1962**, *1*, 893. (c) Deacon, G. B.; Nelson-Reed, K. T. *J. Organomet. Chem.* **1987**, *322*, 257. (d) Nair, R. N.; Golen, J. A.; Rheingold, A. L.; Grotjahn, D. B. *Inorg. Chim. Acta* **2010**, *364*, 272.

(39) (a) Kerrison, S. J. S.; Sadler, P. J. *J. Chem. Soc., Chem. Commun.* **1977**, 861. (b) Fischer, S. J.; Benson, L. M.; Fauq, A.; Naylor, S.; Windebank, A. J. *Neurotoxicology* **2008**, *29*, 444.

(40) (a) Kerrison, S. J. S.; Sadler, P. J. *Inorg. Chim. Acta* **1985**, *104*, 197. (b) Tessier, C.; Rochon, F. D. *Inorg. Chim. Acta* **1999**, *295*, 25. (c) Milanesio, M.; Monti, E.; Gariboldi, M. B.; Gabano, E.; Ravera, M.; Osella, D. *Inorg. Chim. Acta* **2008**, *361*, 2803.

(41) Bertani, R.; Seraglia, R.; Favretto, D.; Michelin, R. A.; Mozzon, M.; Sbovata, S. M.; Sassi, A. *Inorg. Chim. Acta* **2003**, *356*, 357.

(42) Weidlein, J.; Müller, U.; Dehnicke, K. *Schwingungsspektroskopie*; Thieme: Stuttgart, Germany, 1988.

(43) Lallemand, J.-Y.; Soulié, J.; Chottard, J.-C. *J. Chem. Soc., Chem. Commun.* **1980**, 436.

(44) (a) Pregosin, P. S. *Coord. Chem. Rev.* **1982**, *44*, 247. (b) Priqueler, J. R. L.; Butler, I. S.; Rochon, F. D. *Appl. Spectrosc. Rev.* **2006**, *41*, 185.

(45) Berners-Price, S. J.; Appleton, T. G. The Chemistry of Cisplatin in Aqueous Solution. In ref 4a, p 3.

(46) Cui, H.; Goddard, R.; Pörschke, K.-R. *Organometallics* **2011**, *30*, 6241.

(47) (a) Legon, A. C.; Millen, D. J. *Chem. Soc. Rev.* **1987**, *16*, 467. (b) Etter, M. C. *Acc. Chem. Res.* **1990**, *23*, 120. (c) Gilli, G.; Gilli, P. *The Nature of the Hydrogen Bond*; Oxford University Press: Oxford, U.K., 2009.

(48) For the structures of *cis*-(ammine)(amine)$PtCl_2$ complexes, see: (a) Talman, E. G.; Brüning, W.; Reedijk, J.; Spek, A. L.; Veldman, N. *Inorg. Chem.* **1997**, *36*, 854. (b) Chen, Y.; Guo, Z.; Parsons, S.; Sadler, P. J. *Chem. Eur. J.* **1998**, *4*, 672.

(49) (a) Cham, S. T.; Diakos, C. I.; Ellis, L. T.; Fenton, R. R.; Munk, V. P.; Messerle, B. A.; Hambley, T. W. *Dalton Trans.* **2001**, 2769. (b) Ranaldo, R.; Margiotta, N.; Intini, F. P.; Pacifico, C.; Natile, G. *Inorg. Chem.* **2008**, *47*, 2820.

(50) Connick, W. B.; Marsh, R. E.; Schaefer, W. P.; Gray, H. B. *Inorg. Chem.* **1997**, *36*, 913.

(51) Lee, S. S.; Jung, O.-S.; Lee, C. O.; Choi, S. U.; Jun, M.-J.; Sohn, Y. S. *Inorg. Chim. Acta* **1995**, *239*, 133.

(52) Reichardt, C.; Welton, T. *Solvents and Solvent Effects in Organic Chemistry*, 4th ed.; Wiley-VCH: Weinheim, Germany, 2010.

(53) Mueller, H.; Kassack, M. U.; Wiese, M. *J. Biomol. Screening* **2004**, *9*, 506.

(54) The IC_{50} value is typically used as a measure of inhibitory potency and is defined for the MTT assay as the concentration at which 50% of the cell viability is inhibited. pIC_{50} is the negative logarithm of the IC_{50} value.

(55) Eckstein, N.; Servan, K.; Hildebrandt, B.; Pölitz, A.; von Jonquières, G.; Wolf-Kümmeth, S.; Napierski, I.; Hamacher, A.; Kassack, M. U.; Budczies, J.; Beier, M.; Dietel, M.; Royer-Pokora, B.; Denkert, C.; Royer, H.-D. *Cancer Res.* **2009**, *69*, 2996.